SLOPE-DEPENDENT NUCLEAR-SYMMETRY ENERGY WITHIN THE EFFECTIVE SURFACE APPROXIMATION

J.P. Blocki,[1] A.G. Magner,[2] and P. Ring[3]

[1] *National Centre for Nuclear Research, PL-00681 Warsaw, Poland*
[2] *Institute for Nuclear Research, 03680 Kyiv, Ukraine*
[3] *Technical Munich University, D-85747 Garching, Germany*

The effective-surface approximation is extended taking into account derivatives of the symmetry-energy density per particle with respect to the mean particle density. The isoscalar and isovector particle densities in this extended effective-surface approximation are derived. The improved expressions of the surface symmetry energy, in particular, its surface tension coefficients in the sharp-edged proton-neutron asymmetric nuclei take into account important gradient terms of the energy density functional. For most Skyrme forces the surface symmetry-energy constants and the corresponding neutron skins and isovector stiffnesses are calculated as functions of the Swiatecki derivative of the nongradient term of the symmetry-energy density per particle with respect to the isoscalar density. Using the analytical isovector surface-energy constants in the framework of the Fermi-liquid droplet model we find energies and sum rules of the isovector giant-dipole resonance structure in a reasonable agreement with the experimental data, and they are compared with other theoretical approaches.

Keywords: Nuclear binding energy, liquid droplet model, extended Thomas-Fermi approach, nuclear surface energy, symmetry energy, neutron skin thickness, isovector stiffness.

PACS numbers: 21.10.Dr, 21.65.Cd, 21.60.Ev, 21.65.Ef

I. INTRODUCTION

Explicit and accurate analytical expressions for the particle density distributions within the nuclear effective-surface (ES) approximation were obtained in Refs. [1–3]. They take advantage of the saturation properties of nuclear matter in the narrow diffuse-edge region in finite heavy nuclei. The ES is defined as the location of points with a maximal density gradient. An orthogonal coordinate system related locally to the ES is specified by the distance ξ of a given point from the ES and the tangent coordinate η parallel to the ES. Using the nuclear energy-density functional theory, one can simplify the variational condition derived from minimization of the nuclear energy at some fixed integrals of motion in the ξ, η coordinates within the leptodermous approximation. In particular, in the extended Thomas-Fermi (ETF) approach [4], this can be done in sufficiently heavy nuclei for any fixed deformation using the expansion in a small parameter $a/R \sim A^{-1/3} \ll 1$ where a is of the order of the diffuse edge thickness of the nucleus, R is the mean curvature radius of the ES, and A is the number of nucleons. The accuracy of the ES approximation in the ETF approach was checked [3] without spin-orbit (SO) and asymmetry terms by comparing results with those of Hartree-Fock (HF) and other ETF models for some Skyrme forces. The ES approach [3] was also extended by taking into account the SO and asymmetry effects [5–7].

Solutions for the isoscalar and isovector particle densities and energies in the ES (leptodermous) approximation of the ETF approach were applied to analytical calculations of the surface symmetry energy, the neutron skin and isovector stiffness coefficient in the leading order of the parameter a/R [7]. Our results are compared with older investigations [8–11] within the liquid droplet model (LDM) and with more recent works [12–27].

The splitting of the isovector giant-dipole resonances into the main and satellite modes [28] was obtained as a function of the isovector surface-energy constant within the Fermi-liquid droplet (FLD) model [29, 30] in the ES approach. The analytical expressions for the surface symmetry-energy constants have been tested by energies and sum rules of the isovector dipole resonances (IVDR) within the FLD model [31] for some Skyrme forces neglecting derivatives of the nongradient terms in the symmetry-energy density per particle with respect to the mean particle density. The so called pygmy dipole resonances (PDR) below the main IVDR peak as a different phenomenon which might not be the result of splitting of the IVDR were intensively discussed in the literature [12–14, 22–25, 32–35]. They might have a different nature and actually are not related to each other. In the present work, we shall extend the variational effective-surface method accounting for the derivatives introduced by Swiatecki and Myers within the LDM [8] and apply it to the IVDR splitting. Some preliminary results were reported in [36].

In Sec. II, we give an outlook of the basic points of the ES approximation within the density functional theory. The main results for the isoscalar and isovector particle densities are presented in Sec. III emphasizing derivatives of the symmetry energy density per particle. Section IV is devoted to analytical derivations of the symmetry energy in terms of the surface energy coefficient, the neu-

tron skin thickness and the isovector stiffness including these derivatives. Sections V and VI are devoted to the collective dynamical description of the IVDR structure in terms of the response functions and transition densities. Discussions of the results are given in Sec. VII and summarized in Sec. VIII. Some details of our calculations are presented in Appendixes A and B.

II. SYMMETRY ENERGY AND PARTICLE DENSITIES

We start with the nuclear energy E as a functional of the isoscalar (ρ_+) and isovector (ρ_-) densities $\rho_\pm = \rho_n \pm \rho_p$ in the local density approach [4, 37–44]:

$$E = \int \mathrm{d}\mathbf{r}\ \rho_+ \mathcal{E}\left(\rho_+, \rho_-\right), \tag{1}$$

where $\mathcal{E}\left(\rho_+, \rho_-\right)$ is the energy density per particle,

$$\mathcal{E}\left(\rho_+, \rho_-\right) = -b_V + JI^2 + \varepsilon_+(\rho_+) + \varepsilon_-(\rho_+, \rho_-) + \\ + \left(\mathcal{C}_+/\rho_+ + \mathcal{D}_+\right)\left(\nabla\rho_+\right)^2 + \left(\mathcal{C}_-/\rho_+ + \mathcal{D}_-\right)\left(\nabla\rho_-\right)^2. \tag{2}$$

Here, $b_V \approx 16$ MeV is the separation energy of a particle, $J \approx 30$ MeV is the main volume symmetry-energy constant of infinite nuclear matter, and $I = (N-Z)/A$ is the asymmetry parameter; $N = \int \mathrm{d}\mathbf{r}\rho_n(\mathbf{r})$ and $Z = \int \mathrm{d}\mathbf{r}\rho_p(\mathbf{r})$ are the neutron and proton numbers, and $A = N + Z$. These constants determine the first two terms of the volume energy. The last four terms are surface terms. The first two terms are independent of the gradients of the particle densities and the last two depend on these gradients. For the first surface term independent of the gradients, ε_+, one obtains

$$\varepsilon_+(\rho_+) = \frac{K_+}{18}\ e_+\left[\epsilon(w_+)\right], \tag{3}$$

where $K_+ \approx 215 - 245$ MeV (see Table I) is the isoscalar in-compressibility modulus of symmetric nuclear matter, w_+ is the dimensionless isoscalar particle density, $w_+ = \rho_+/\overline{\rho}$ and

$$e_+\left[\epsilon\left(w_+\right)\right] = 9\epsilon^2 + I^2\left[\mathcal{S}_{\mathrm{sym}}(\epsilon) - J\right]/K_+ \tag{4}$$

with

$$\epsilon = \frac{\overline{\rho} - \rho_+}{3\overline{\rho}} = \frac{1 - w_+}{3}. \tag{5}$$

ϵ is the small parameter in the expansion,

$$\mathcal{S}_{\mathrm{sym}}(\epsilon) = J - L\epsilon + \frac{K_-}{2}\epsilon^2 + ..., \tag{6}$$

around the particle density of infinite nuclear matter $\overline{\rho} = 3/4\pi r_0^3 \approx 0.16$ fm^{-3} and r_0 is the commonly accepted constant in the $A^{1/3}$ dependence of a mean radius. Several other quantities, which were introduced by Myers and Swiatecki [8], will be explained below. The derivative corrections of $\mathcal{S}_{\mathrm{sym}}(\epsilon)$ in Eq. (6) were neglected in our previous calculations [7]. The next isovector surface term $\varepsilon_-(\rho_+, \rho_-)$ can be defined through the same function $\mathcal{S}_{\mathrm{sym}}(\epsilon)$ in Eq. (6):

$$\varepsilon_-\left(\rho_+, \rho_-\right) = \mathcal{S}_{\mathrm{sym}}(\epsilon)\ \left(\frac{\rho_-}{\rho_+}\right)^2 - JI^2. \tag{7}$$

For the first and second derivatives of $\mathcal{S}_{\mathrm{sym}}(\epsilon)$ with respect to ϵ one can take in Eq. (6) the values $L \approx 20 \div 120$ MeV and, even less known, K_- [19, 27, 45]. The constants $\mathcal{C}_\pm$ and $\mathcal{D}_\pm$ in Eq. (2) are defined by the parameters of the Skyrme forces [4, 37, 39, 41, 43],

$$\mathcal{C}_+ = \frac{1}{12}\left(t_1 - \frac{25}{12}t_2 - \frac{5}{3}t_2x_2\right), \tag{8}$$
$$\mathcal{C}_- = -\frac{t_1}{48}\left(1 + \frac{5}{2}x_1\right) - \frac{t_2}{36}\left(1 + \frac{19}{8}x_2\right).$$

The isoscalar SO gradient terms in (2) are defined with a constant: $\mathcal{D}_+ = -9mW_0^2/16\hbar^2$, where $W_0 \approx 100$–130 MeV·fm^5 and m is the nucleon mass. The constant $\mathcal{D}_-$ is usually relatively small and will be neglected below for simplicity. Equation (2) can be applied in a semiclassical approximation for a realistic Skyrme force [37, 39–42], in particular by neglecting higher $\hbar$ corrections in the ETF kinetic energy [2–4] and also Coulomb terms. All of them easily were taken into account [1, 5] neglecting relatively small Coulomb exchange terms. Such exchange terms can be calculated numerically in extended Slater approximations [46].

The energy density per particle in Eq. (2) contains the first two volume terms and surface components including the new L and K_- derivative corrections ε_- (in contrast to Ref. [7]) and also the isoscalar and isovector density gradients. Both are important for finite nuclear systems. These gradient terms together with the other surface components in the energy density within the ES approximation are responsible for the surface tension in finite nuclei.

As usual, we minimize the energy E under the constraints of fixed particle number $A = \int \mathrm{d}\mathbf{r}\ \rho_+(\mathbf{r})$ and neutron excess $N - Z = \int \mathrm{d}\mathbf{r}\ \rho_-(\mathbf{r})$ using the Lagrange multipliers λ_+ and λ_-, the isoscalar and isovector chemical-potential surface corrections (see Appendix A). Taking also into account additional deformation constraints (like the quadrupole moment), our approach can be applied for any deformation parameter of the nuclear surface, if its diffuseness a is small with respect to the curvature radius R. Approximate analytical expressions of the binding energy will be obtained at least up to order $A^{2/3}$. To satisfy the condition of particle number conservation with the required accuracy we account for relatively small surface corrections ($\propto a/R \sim A^{-1/3}$ in first order) to the leading terms in the Lagrange multipliers [2, 3, 5, 7] (see Appendix B). We take into account explicitly the diffuseness of the particle density distributions. Solutions of the variational Lagrange equations can be derived analytically for the isoscalar and isovector surface tension coefficients (energy constants), instead of the phenomenological constants of the standard LDM [8] (the neutron

and proton particle densities were considered earlier to be distributions with a strictly sharp edge).

III. EXTENDED ISOSCALAR AND ISOVECTOR DENSITIES

For the isoscalar particle density, $w = \rho_+/\overline{\rho}$, one has up to the leading terms in the leptodermous parameter a/R the usual first-order differential Lagrange equation [3, 5, 7]. Integrating this equation, one finds the solution:

$$x = -\int_{w_r}^{w} \mathrm{d}y \, \sqrt{\frac{1+\beta y}{y\; e_+[\epsilon(y)]}}\;, \qquad x = \frac{\xi}{a}, \tag{9}$$

for $x < x(w=0)$ and $w = 0$ for $x \geq x(w=0)$, where $x(w=0)$ is the turning point. $\beta = \mathcal{D}_+\overline{\rho}/\mathcal{C}_+$ is the dimensionless SO parameter, see Eq. (4) for $e_+[\epsilon(y)]$ (for convenience we often omit the lower index "+" in w_+). For $w_r = w(x=0)$, one has the boundary condition, $\mathrm{d}^2w(x)/\mathrm{d}x^2 = 0$ at the ES ($x = 0$):

$$e_+[\epsilon(w_r)] + w_r(1+\beta w_r)\left[\frac{\mathrm{d}e_+[\epsilon(w)]}{\mathrm{d}w}\right]_{w=w_r} = 0\;. \tag{10}$$

In Eq. (9), $a \approx 0.5-0.6$ fm is the diffuseness parameter [7],

$$a = \sqrt{\frac{\mathcal{C}_+\overline{\rho}K_+}{30b_V^2}}, \tag{11}$$

found from the asymptotic behavior of the particle density, $w \sim \exp(-\xi/a)$ for large ξ ($\xi \gg a$).

As shown in Refs. [3, 5], the influence of the semiclassical $\hbar$ corrections (related to the ETF kinetic energy) to $w(x)$ is negligibly small everywhere, except for the quantum tail outside the nucleus ($x \gtrsim 1$). Therefore, all these corrections were neglected in Eq. (2). With a good convergence of the expansion of the $e_+[\epsilon(y)]$ in powers of $1-y$ up to the leading quadratic term [3, 5] and small I^2 corrections in Eq. (4), $e = (1-y)^2$, one finds analytical solutions of Eq. (9) in terms of the algebraic, trigonometric and logarithmic functions [7]. For $\beta = 0$ (i.e. without SO terms), it simplifies to the solution $w(x) = \tanh^2[(x-x_0)/2]$ for $x \leq x_0 = 2\mathrm{arctanh}(1/\sqrt{3})$ and zero for x outside the nucleus ($x > x_0$).

After simple transformations of the isovector Lagrange equation (A1) one similarly finds up to the leading term in a/R in the ES approximation for the isovector density, $w_-(x) = \rho_-/(\overline{\rho}I)$, the equation and the boundary condition (A3). The analytical solution $w_- = w\cos[\psi(w)]$ can be obtained through the expansion (A5) of ψ in powers of

$$\gamma(w) = \frac{3\epsilon}{c_{\mathrm{sym}}}, \qquad c_{\mathrm{sym}} = a\,\sqrt{\frac{J}{\overline{\rho}\;|\mathcal{C}_-|}}\;. \tag{12}$$

Expanding up to the second order in γ one obtains (see Appendix A)

$$w_- = w\,\cos[\psi(w)] \approx w\left(1 - \frac{\psi^2(w)}{2} + ...\right), \tag{13}$$

with

$$\psi(w) = \frac{\gamma(w)}{\sqrt{1+\beta}}\;\left[1 + \widetilde{c}\gamma(w) + ...\right], \tag{14}$$

$$\widetilde{c} = \frac{\beta c_{\mathrm{sym}}^2 + 2 + c_{\mathrm{sym}}^2 L(1+\beta)/(3J)}{2c_{\mathrm{sym}}(1+\beta)}, \tag{15}$$

[see also the constant c_3 (Appendix A) at higher (third) order corrections]. The constant $\widetilde{c}$ [Eq. (15)] for the isovector solutions w_-, Eq. (13), is modified with respect to Ref. [7] in two aspects. In addition to the L dependence there are also higher order terms from a nonlinear equation (A4) for $\psi(w)$ (Appendix A). Notice also that w_- depends on L in second order in γ but it is independent of K_- at this order (Appendix A).

In Fig. 1, the L dependence of the function $w_-(x)$ is shown within the total interval from $L = 0$ to $L = 100$ MeV [20] and it is compared to that of the density $w(x)$ for the SLy5* force as a typical example. As shown in Fig. 2 in a larger (logarithmic) scale, one observes notable differences in the isovector densities w_- derived from different Skyrme forces [37, 41] within the edge diffuseness. All these calculations have been done with the finite proper value of the slope parameter L. For SLy forces this value is taken from Ref. [44], for *SGII* from Ref. [20] and for others from Ref. [41] (Table I). As shown below, this is in particular important for calculations of the neutron skin of nuclei. Notice that, with the precision of line thickness, our results are almost the same taking approximately $L = 50$ MeV for SLy5* and $L = 60$ MeV for SVsym32. Note also that, up to second order in the small parameter γ, the isovector particle density w_- in Eq. (13) does not depend on the symmetry-energy incompressibility K_-. The K_- dependence appears only at higher (third) order terms in the expansion in γ (Appendix A). Therefore, as a first step of the iteration procedure, it is possible to study first the main slope effects of L neglecting small I^2 corrections to the isoscalar particle density w_+ (9) through e_+ (4). Then, we may study more precisely the effect of the second derivatives K_- taking into account higher order terms.

We emphasize that the dimensionless densities, $w(x)$ [see Eq. (9) and Ref. [7]] and $w_-(x)$ (13), shown in Figs. 1 and 2, were obtained in leading ES approximation ($a/R \ll 1$) as functions of specific combinations of Skyrme force parameters like β and c_{sym} [Eq. (12)] accounting for the L-dependence [Eq. (15)]. These densities are at the leading order in the leptodermous parameter a/R approximately universal functions, independent of the properties of the specific nucleus. It yields largely the local density distributions in the normal-to-ES direction ξ with the correct asymptotic behavior outside

of the deformed ES layer at $a/R \ll 1$, as is the case for semi-infinite nuclear matter. Therefore, at the dominating order, the particle densities $w_\pm$ are universal distributions independent of the specific properties of nuclei while higher order corrections to the densities $w_\pm$ depend on the specific macroscopic properties of nuclei.

IV. ISOVECTOR ENERGY AND STIFFNESS

The nuclear energy E [Eq. (1)] in the improved ES approximation (Appendix B) is split into volume and surface terms [7],

$$E \approx -b_V\, A + J(N-Z)^2/A + E_S\,. \tag{16}$$

For the surface energy E_S one obtains

$$E_S = E_S^{(+)} + E_S^{(-)} \tag{17}$$

with the isoscalar (+) and isovector (-) surface components:

$$E_S^{(\pm)} = b_S^{(\pm)} \frac{\mathcal{S}}{4\pi r_0^2}, \tag{18}$$

where $\mathcal{S}$ is the surface area of the ES, $b_S^{(\pm)}$ are the isoscalar (+) and isovector (−) surface-energy constants,

$$b_S^{(\pm)} \approx 8\pi r_0^2 \mathcal{C}_\pm \int_{-\infty}^{\infty} \mathrm{d}\xi \, \left(1 + \frac{\mathcal{D}_\pm}{\mathcal{C}_\pm}\rho_+\right)\left(\frac{\partial \rho_\pm}{\partial \xi}\right)^2. \tag{19}$$

These constants are proportional to the corresponding surface tension coefficients $\sigma_\pm = b_S^{(\pm)}/(4\pi r_0^2)$ through the solutions (9) and (13) for $\rho_\pm(\xi)$ which can be taken into account in leading order of a/R (Appendix B). These coefficients $\sigma_\pm$ are the same as found in the expressions for the capillary pressures of the macroscopic boundary conditions [see Ref. [7] with new values $\varepsilon_\pm$ modified by L and K_- derivative corrections of Eqs. (4) and (7)]. Within the improved ES approximation where also higher order corrections in the small parameter a/R are taken into account, we derived in Ref. [7] equations for the nuclear surface itself (see also Refs. [2, 3, 5]). For more exact isoscalar and isovector particle densities we account for the main terms in the next order of the parameter a/R in the Lagrange equations (see Eq. (A1) for the isovector and Refs. [2, 3, 5] for the isoscalar case). Multiplying these equations by $\partial\rho_-/\partial\xi$ and integrating them over the ES in the normal-to-surface direction ξ and using the solutions for $w_\pm(x)$ up to the leading orders [Eqs. (9) and (13)], one arrives at the ES equations in the form of the macroscopic boundary conditions [2, 3, 5, 7, 30, 47–49]. They ensure equilibrium through the equivalence of the volume and surface (capillary) pressure variations. As shown in Ref. [7], the latter ones are proportional to the corresponding surface tension coefficients $\sigma_\pm$.

For the energy surface coefficients $b_S^{(\pm)}$ (19), one obtains

$$b_S^{(+)} = 6\mathcal{C}_+\overline{\rho}\mathcal{J}_+/(r_0 a),$$
$$\mathcal{J}_+ = \int_0^1 \mathrm{d}w \sqrt{w(1+\beta w)\; e_+[\epsilon(w)]}, \tag{20}$$

$$b_S^{(-)} = k_S\, I^2, \qquad k_S = 6\overline{\rho}\,\mathcal{C}_-\,\mathcal{J}_-/(r_0 a), \tag{21}$$

$$\mathcal{J}_- = \int_0^1 \mathrm{d}w \,\sqrt{\frac{w\; e_+[\epsilon(w)]}{1+\beta w}}$$
$$\times \left\{\cos(\psi) + \frac{w\sin(\psi)}{c_{\rm sym}\sqrt{1+\beta}}\,[1 + 2\widetilde{c}\gamma(w)]\right\}^2$$
$$\approx \int_0^1 (1-w)\mathrm{d}w\,\sqrt{\frac{w}{1+\beta w}}\,\left\{1 + \frac{2\gamma(w)}{c_{\rm sym}(1+\beta)}\right.$$
$$\left. + \left(\frac{\gamma}{1+\beta}\right)^2\left[\frac{1}{c_{\rm sym}^2} + 6(1+\beta)\left(\frac{\widetilde{c}}{c_{\rm sym}} - \frac{1}{2}\right)\right]\right\}. \tag{22}$$

For γ and $\widetilde{c}$, see Eqs. (12) and (15), respectively. Simple expressions for the constants $b_S^{(\pm)}$ in Eqs. (20) and (21) can be easily derived in terms of algebraic and trigonometric functions by calculating explicitly integrals over w for the quadratic form of $e_+[\epsilon(w)]$ [Eqs. (B3) and (B5)]. Note that in these derivations, we neglected curvature terms and, being of the same order, shell corrections, which have been discarded from the very beginning. The isovector energy terms were obtained within the ES approximation with high accuracy up to the product of two small quantities, I^2 and $(a/R)^2$.

According to the macroscopic theory [7–10], one may define the isovector stiffness Q with respect to the difference $R_n - R_p$ between the neutron and proton radii as a dimensionless collective variable τ,

$$E_s^{(-)} = -\frac{\overline{\rho} r_0}{3}\oint \mathrm{d}S\, Q\tau^2 \approx -\frac{Q\tau^2\mathcal{S}}{4\pi r_0^2},$$
$$\tau = (R_n - R_p)/r_0\,, \tag{23}$$

where τ is the relative neutron skin. Comparing this expression to Eq. (18) for the isovector surface energy written through the isovector surface-energy constant $b_S^{(-)}$ [Eq. (21)], one obtains

$$Q = -k_S\frac{I^2}{\tau^2}\,. \tag{24}$$

Defining the neutron and proton radii $R_{n,p}$ as positions of maxima of the neutron and proton density gradients, respectively, one obtains the neutron skin τ (Ref. [7]),

$$\tau = \frac{8aI}{r_0 c_{\rm sym}^2} g(w_r), \tag{25}$$

where

$$g(w)=\frac{w^{3/2}(1+\beta w)^{5/2}}{(1+\beta)(3w+1+4\beta w)}\ \left\{w(1+2\widetilde{c}\gamma)^2 + 2\gamma\,(1+\widetilde{c}\gamma)\,[\widetilde{c}w-c_{\rm sym}\,(1+2\widetilde{c}\gamma)]\right\} \quad (26)$$

is taken at the ES value w_r [Eq. (10)]. Finally taking into account Eqs. (24) and (21), one arrives at

$$Q=-\nu\,\frac{J^2}{k_{_S}},\qquad \nu=\frac{k_{_S}^2I^2}{\tau^2J^2}=\frac{9\mathcal{J}_-^2}{16g^2(w_r)}, \quad (27)$$

where $\mathcal{J}_-$ and $g(w)$ are given by Eqs. (22) and (26), respectively. Note that $Q=-9J^2/4k_{_S}$ was predicted in Refs. [8, 9] and therefore for $\nu=9/4$ the first part of (27) which relates Q with the volume symmetry energy J and the isovector surface-energy constant $k_{_S}$, is identical to that used in Refs. [8–11, 19, 20]. However, in our derivations ν deviates from 9/4 and it is proportional to the function $\mathcal{J}_-^2/g^2(w_r)$. This function depends significantly on the SO interaction parameter β but not too much on the specific Skyrme force (see Ref. [7] for details).

Notice that the approximate universal functions $w(x)$ [Eq. (9) and Ref. [7]] and $w_-(x)$ [Eq. (13)] can be used in the leading order of the ES approximation for calculations of the surface energy coefficients $b_{_S}^{(\pm)}$ [Eq. (19)] and the neutron skin $\tau\propto I$ [Eq. (25)]. As shown in Ref. [7] and in Appendix B, here only the particle density distributions $w(x)$ and $w_-(x)$ are needed within the surface layer through their derivatives [the lower limit of the integration over ξ in Eq. (19) can be approximately extended to $-\infty$ because there are no contributions from the internal volume region in the evaluation of the main surface terms of the pressure and energy]. Therefore, the surface symmetry-energy coefficient $k_{_S}$ in Eqs. (21) and (B5) , the neutron skin τ [Eq. (25)] and the isovector stiffness Q [Eq. (27)] can be approximated analytically in terms of functions of definite critical combinations of the Skyrme parameters like β, $c_{\rm sym}$, a, $\mathcal{C}_-$ and parameters of infinite nuclear matter ($b_{\rm V}$, $\overline{\rho}$, K_+), also the symmetry energy constants J, L and K_-. Thus, in the considered ES approximation, they do not depend on the specific properties of the nucleus (for instance, the neutron and proton numbers), the curvature and the deformation of the nuclear surface.

V. THE FERMI-LIQUID DROPLET MODEL

For IVDR calculations, the FLD model based on the linearized Landau-Vlasov equations for the isoscalar $[\delta f_+(\mathbf{r},\mathbf{p},t)]$ and isovector $[\delta f_-(\mathbf{r},\mathbf{p},t)]$ distribution functions can be used in phase space [30, 50, 51],

$$\frac{\partial\delta f_\pm}{\partial t}+\frac{\mathbf{p}}{m_\pm^*}\nabla_r\left[\delta f_\pm + \delta\,(e-e_{_F})\left(\delta V_\pm+V_{\rm ext}^\pm\right)\right]=\delta St_\pm. \quad (28)$$

Here $e=p^2/(2m_\pm^*)$ is the equilibrium quasiparticle energy ($p=|\mathbf{p}|$) and $e_{_F}=(p_F^\pm)^2/(2m_\pm^*)$ is the Fermi energy. The isotopic dependence of the Fermi momenta $p_F^\pm=p_{_F}\,(1\mp\Delta)$ is given by a small parameter $\Delta=2\,(1+F_0')\ I/3$. The reason for having Δ is the difference between the neutron and proton potential depths from the Coulomb interaction. The isotropic isoscalar F_0 and isovector F_0' Landau interaction constants are related to the isoscalar in-compressibility $K=6e_{_F}(1+F_0)$ and the volume symmetry energy $J=2e_{_F}(1+F_0')/3$ constants of nuclear matter, respectively. The effective masses $m_+^*=m(1+F_1/3)$ and $m_-^*=m(1+F_1'/3)$ are determined in terms of the nucleon mass m by anisotropic Landau constants F_1 and F_1'. Equations (28) are coupled by the dynamical variation of the quasiparticles' selfconsistent interaction $\delta V_\pm$ with respect to the equilibrium value $p^2/(2m_\pm^*)$. The time-dependent external field $V_{\rm ext}^\pm\propto\exp(-i\omega t)$ is periodic with a frequency ω. For simplicity, the collision term $\delta St_\pm$ is calculated within the relaxation time $\mathcal{T}(\omega)$ approximation accounting for the retardation effects from the energy-dependent self-energy beyond the mean field approach, $\mathcal{T}=4\pi^2\mathcal{T}_0/(\hbar\omega)^2$ with the parameter $\mathcal{T}_0\propto A^{-1/3}$ [see Eq. (80) of Ref. [51] at zero temperature and also Ref. [30]].

The solutions of Eq. (28) are related to the dynamic multipole particle-density variations, $\delta\rho_\pm(\mathbf{r},t)\propto Y_{\lambda0}(\hat{r})$, where $Y_{\lambda0}(\hat{r})$ are the spherical harmonics and $\hat{r}=\mathbf{r}/r$. These solutions can be found in terms of the superposition of plane waves over the angle of a wave vector $\mathbf{q}$,

$$\delta f_\pm(\mathbf{p},\mathbf{r},t)=\int \mathrm{d}\Omega_{\mathbf{q}}Y_{\lambda0}(\hat{q})\ \delta f_\pm(\mathbf{p},\mathbf{q},\omega) \times\exp\left[-i\,(\omega t-\mathbf{qr})\right], \quad (29)$$

where $\delta f_\pm(\mathbf{p},\mathbf{q},\omega)$ is the Fourier transform of the distribution function. The time-dependence (29) is periodic as the external field $V_{\rm ext}^\pm$ is also periodic with the same frequency $\omega=p_{_F}^\pm s^\pm q/m_\pm^*$ where $s^+=s$, and $s^-=s\left(NZ/A^2\right)^{1/2}$. The factor $\left(NZ/A^2\right)^{1/2}$ accounts for conserving the position of the mass center for the isovector vibrations [53]. The sound velocity s can be found from the dispersion equations [30]. The two solutions s_n with $n=1,2$ are functions of the Landau interaction constants and $\omega\mathcal{T}$. Due to the symmetry interaction coupling the "out-of-phase" particle-density vibrations of the s_1 mode involve the "in-phase" mode s_2 inside of the nucleus.

For small isovector and isoscalar multipole ES-radius vibrations of the finite neutron and proton Fermi-liquid drops around the spherical nuclear shape, one has $\delta R_\pm(t)=R\alpha_{_S}^\pm(t)Y_{\lambda0}(\hat{r})$ with a small time-dependent amplitudes $\alpha_{_S}^\pm(t)=\alpha_{_S}^\pm\exp(-i\omega t)$. The macroscopic boundary conditions (surface continuity and force-equilibrium equations) at the ES are given by Refs. [7, 30, 51]:

$$u_r^\pm\Big|_{r=R}=R\dot{\alpha}_{_S}^\pm Y_{\lambda0}(\hat{r}),$$
$$\delta\Pi_{rr}^\pm\Big|_{r=R}=\alpha_{_S}^\pm\overline{P}_{_S}^\pm\ Y_{\lambda0}(\hat{r}). \quad (30)$$

The left hand sides of these equations are the radial components of the mean-velocity field $\mathbf{u} = \mathbf{j}/\rho$ ($\mathbf{j}$ is the current density) and the momentum flux tensor $\delta\Pi_{\nu\mu}$ defined both through the moments of $\delta f(\mathbf{r}, \mathbf{p}, t)$ in momentum space [30, 51]. The right-hand sides of Eq. (30) are the ES velocities and capillary pressures. These pressures are proportional to the isoscalar and isovector surface-energy constants $b_S^{\pm}$ in Eq. (19),

$$\overline{P}_S^{\pm} = \frac{2}{3}\, b_S^{\pm}\, \overline{\rho}\, \mathcal{P}_{\pm}\, A^{\mp 1/3}, \tag{31}$$

where $\mathcal{P}_+ = (\lambda - 1)(\lambda + 2)/2$, $\mathcal{P}_- = 1$. The coefficients $b_S^{\pm}$ are essentially determined by the constants $\mathcal{C}_{\pm}$ [Eq. (8)] of the energy density (2) in front of its gradient density terms. The conservation of the center of mass is taken into account in the derivations of the second boundary conditions (30) [30, 51]. Therefore, one has a dynamical equilibrium of the forces acting at the ES.

VI. TRANSITION DENSITY AND NUCLEAR RESPONSE

The response function, $\chi_{\pm}(\omega)$, is defined as a linear reaction to the external single particle field $\hat{F}(\mathbf{r})$ with the frequency ω. For convenience, we may consider this field in terms of a similar superposition of plane waves (29) as $\delta f_{\pm}$ [30, 51]. In the following, we will consider the long wave-length limit with $\mathcal{V}_{\rm ext}^{\pm}(\mathbf{r}, t) = \alpha_{\rm ext}^{\pm,\omega}(t)\hat{F}(\mathbf{r})$ and $\alpha_{\rm ext}^{\pm,\omega}(t) = \alpha_{\rm ext}^{\pm,\omega}\, e^{-i(\omega + i\eta_o)t}$, where $\alpha_{\rm ext}^{\pm,\omega}$ is the amplitude and ω is the frequency of the external field ($\eta_o = +0$). In this limit, the one-body operator $\hat{F}(\mathbf{r})$ becomes the standard multipole operator, $\hat{F}(\mathbf{r}) = r^{\lambda} Y_{\lambda 0}(\hat{r})$ for $\lambda \geq 1$. The response function $\chi_{\pm}(\omega)$ is expressed through the Fourier transform of the transition density $\rho_{\pm}^{\omega}(\mathbf{r})$ as

$$\chi_{\pm}(\omega) = -\int \mathrm{d}\mathbf{r}\ \hat{F}(\mathbf{r})\ \rho_{\pm}^{\omega}(\mathbf{r})/\alpha_{\rm ext}^{\pm,\omega}. \tag{32}$$

The transition density $\rho_{\pm}^{\omega}(\mathbf{r})$ is obtained through the dynamical part of the particle density $\delta\rho_{\pm}(\mathbf{r}, t)$ in a macroscopic model in terms of solutions $\delta f_{\pm}(\mathbf{r}, \mathbf{p}, t)$ of the Landau-Vlasov equations (28) with the boundary conditions (30) as the same superpositions of plane waves (29) [30]: $\delta\rho_-(\mathbf{r}, t) = \overline{\rho}\ \alpha_S^-\rho_-^{\omega}(x)\ Y_{10}(\hat{r})\ e^{-i\omega t}$, where

$$\rho_-^{\omega}(x) = \frac{qR}{j_1'(qR)}\left[j_1(\kappa)\, w(x) + \frac{g_{_V}}{g_{_S}}\frac{\mathrm{d}w_-}{\mathrm{d}x}\right], \tag{33}$$

$$g_{_V} = \int_0^{w_0} \mathrm{d}w \frac{\sqrt{w(1+\beta w)}}{1-w}\kappa^3 j_1(\kappa), \tag{34}$$

$$g_{_S} = \int_0^{w_0} \mathrm{d}w\ \kappa^3\left[1 + \mathcal{O}(\gamma^2(w))\right], \tag{35}$$

$$\kappa = \kappa_o\left[1 + \frac{a}{R}x(w)\right], \tag{36}$$

$\kappa_o = qR$. The first term in (33), proportional to the dimensionless isoscalar density $w(x)$ (in units of $\overline{\rho}$) accounts for volume density vibrations [Eq. (9)]. The second term $\propto dw_-/dx$, where w_- is a dimensionless isovector density (in units of $\overline{\rho}I$) corresponds to the density variations from a shift of the ES [Eq. (13)]. The particle number and the center-of-mass position are conserved, and $j_\lambda(\kappa)$ and $j_\lambda'(\kappa)$ are the spherical Bessel functions and their derivatives. The upper integration limit $w_{_0}$ in Eqs. (34) and (35) is defined as the root of a transcendent equation $x(w_0) + R/a = 0$. As shown in Appendix A, the SO and L dependent density $w_-(x)$ is of the same order as $w(x)$. The dependencies of $w_-(x)$ on different Skyrme force parameters, mostly the isovector gradient-term constant $\mathcal{C}_-$, the SO parameter β, and the derivative of the volume symmetry energy L are the main reasons for the different values of the neutron skin.

With the help of the boundary conditions (30), one can derive the response function (32) [30],

$$\chi_\lambda(\omega) = \sum_n \chi_\lambda^{(n)}(\omega) = \sum_n \mathcal{A}_\lambda^{(n)}(\kappa_o)/\mathcal{D}_\lambda^{(n)}\left(\omega - i\frac{\Gamma}{2}\right), \tag{37}$$

with $\omega = p_F s_n \kappa_o \left(NZ/A^2\right)^{1/2}/(m^* R)$ ($m_-^* \approx m_+^* = m^*$). This response function describes two modes, the main ($n = 1$) IVDR and its satellite ($n = 2$) as related to the out-of-phase s_1 and in-phase s_2 sound velocities which are excited in the nuclear volume, respectively. We assume here that the "main" peak exhausts mostly the energy weighted sum rule (EWSR) and the "satellite" corresponds to a much smaller part of the EWSR as proportional to the asymmetry parameter, $I \ll 1$. This two-peak structure is from the coupling of the isovector and isoscalar density-volume vibrations because of the neutron and proton quasiparticle interaction $\delta V_{\pm}$ in Eq. (28). Therefore, one takes into account an admixture of the isoscalar mode to the isovector IVDR excitation. The wave numbers $q = \kappa_o/R$ of the lowest poles ($n = 1, 2$) in the response function (37) are determined by the secular equation,

$$\mathcal{D}_\lambda^{(n)} \equiv j_\lambda'(\kappa_o) - \frac{3e_{_F}\kappa_o c_1^{(n)}}{2b_S^- A^{1/3}}\left[j_\lambda(\kappa_o) + c_2^{(n)} j_\lambda''(\kappa_o)\right] = 0. \tag{38}$$

The width of an IVDR peak Γ in (37) corresponds to an imaginary part of the pole having its origin in the collision term $\delta St_{\pm}$ of the Landau-Vlasov equation. At this pole, for the relaxation time one has

$$\mathcal{T}_n = 4\pi^2\mathcal{T}_0/(\hbar\omega_n)^2 \tag{39}$$

with an A-dependent constant, $\mathcal{T}_0 \propto A^{-1/3}$. For the amplitudes one has $\mathcal{A}_\lambda^{(n)} \propto \Delta^{n-1}$. The complete expressions for the amplitudes $\mathcal{A}_\lambda^{(n)}$ and the constants $c_i^{(n)}$ are given in Refs. [30, 51]. Assuming a small value of Δ, one may call the $n = 2$ mode a "satellite" to the "main" $n = 1$ peak. On the other hand, other factors such as a collisional relaxation time, the surface symmetry-energy

constant b_S^-, and the particle number A lead sometimes to a re-distribution of the EWSR values among these two IVDR peaks. The slope L dependence of the transition densities $\rho_-^\omega(x)$ [Eq. (33)] and the strength of the response function,

$$S(\omega) = \mathrm{Im}\chi_\lambda(\omega)/\pi \tag{40}$$

[Eq. (37)] has its origin in the symmetry-energy coefficient $b_S^{(-)}$ [Eqs. (21), (22), (15), (4) and (6)]. Thus, one may evaluate the EWSR sum rule contribution of the nth peak by integration over the region around the peak energy $E_n = \hbar\omega_n$,

$$S_n^{(1)} = \hbar^2 \int \mathrm{d}\omega\ \omega\ S_n(\omega). \tag{41}$$

In accordance with the time-dependent HF approaches based on the Skyrme forces, (see, for instance, [24, 25, 28]), we may expect that the energies of the satellite resonances in the IVDR and ISDR channels can be close. Therefore, we may calculate separately the neutron, $\rho_n^\omega(x)$, and proton, $\rho_p^\omega(x)$, transition densities for the satellite by calculating the isovector and isoscalar transition densities at the same energy E_2 and in the same units as $\rho_\pm$,

$$\rho_n^\omega(x) = \frac{\rho_+^\omega(x) + \rho_-^\omega(x)}{2}, \quad \rho_p^\omega(x) = \frac{\rho_+^\omega(x) - \rho_-^\omega(x)}{2}. \tag{42}$$

VII. DISCUSSION OF THE RESULTS

In Table II we show the isovector surface energy coefficient k_S [Eq. (21)], the stiffness parameter Q [Eq. (27)], its constant ν and the neutron skin τ [Eq. (25)] for many more Skyrme forces than discussed in [36]. They are obtained within the ES approximation with the quadratic expansion for $e_+[\epsilon(w)]$ and neglecting the I^2 slope corrections, for several Skyrme forces [37, 41] whose parameters are presented in Table I. Also shown are the quantities k_{S0}, ν_0, Q_0 and τ_0 neglecting the slope corrections ($L = 0, K_- = 0$). This is in addition to results of Ref. [7] where another important dependence on the SO interaction measured by β was presented. In contrast to a fairly good agreement for the analytical isoscalar surface-energy constant $b_S^{(+)}$ (20) as shown in Ref. [7] and references cited therein, the isovector energy coefficient k_S is more sensitive to the choice of the Skyrme forces than the isoscalar one $b_S^{(+)}$ [Eq. (20) and Ref. [5]]. The modulus of k_S is significantly larger for most of the Skyrme forces SLy... [37] and SV... [41] than for the other ones. However, the L dependence of k_S is somewhat small in these forces (cf. the first two rows of Table II) as it should be for a small parameter ϵ of the symmetry-energy density expansion (6). For SLy and SV forces, the stiffnesses Q are correspondingly significantly smaller in absolute value being closer to the well-known empirical values $Q \approx 30 - 35$ MeV [9–11] obtained by Swiatecki and collaborators. Note that the isovector stiffness Q is even much more sensitive to the parametrization of the Skyrme force and to the slope parameter L than the constants k_S. In Ref. [7], we studied the hydrodynamical results for Q as compared to the FLD model for the averaged properties of the giant IVDR (IVGDR) at zero slope $L = 0$. The IVDR structure in terms of the two (main and satellite) peaks was discussed earlier in Refs. [31] at $L = 0$ in some magic nuclei with a large neutron excess within the semiclassical FLD model based on the effective surface approach. For the comparison with experimental data and other theoretical results we present in Table II (row 9 and 11) a small L dependence of the IVGDR energy parameter $D = E_{\mathrm{IVGDR}} A^{1/3}$, where $E_{\mathrm{IVGDR}} = [E_1 S_1 + E_2 S_2] / [S_1 + S_2]$ is the IVGDR energy for the isotope ^{132}Sn [$S_n = S(\omega_n)$, see also Eq. (40) for the definition of the strength $S(\omega)$]. A more precise reproduction of the A-dependence of the IVGDR energy parameter D for finite values of L (see the last three rows for several isotopes) might determine more consistent values of Q, but, at present, it seems to be beyond the accuracy of both the hydrodynamical and the FLD models. The IVGDR energies obtained by the semiclassical Landau-Vlasov equation (28) with the macroscopic boundary conditions (30) of the FLD model (Ref. [7]) are also basically insensitive to the isovector surface energy constant k_S [6, 7, 31, 36]. They are in a good agreement with the experimental data, and do not depend much on the Skyrme forces even if we take into account the slope symmetry-energy parameter L (last three rows in Table II).

More realistic self-consistent HF calculations taking into account the Coulomb interaction, the surface curvature, and quantum shell effects have led to larger values of $Q \approx 30 - 80$ MeV [4, 20]. For larger Q (see Table II) the fundamental parameter $(9J/4Q)A^{-1/3}$ of the LDM expansion in Ref. [8] is really small for $A \gtrsim 40$, and therefore, the results obtained using the leptodermous expansion are better justified.

An investigation within the approach presented in Sec. V shows that the IVDR strength is split into a main peak which exhausts an essential part of the EWSR independent of the model and a satellite peak with a much smaller contribution to this quantity. Focusing on a much more sensitive k_S dependence of the IVDR satellite resonances, one may take now into account the slope L dependence of the symmetry-energy density per particle (6) (Refs. [22–25] and [31]). The total IVDR strength function being the sum of the "out-of-phase" $n = 1$ and "in-phase" $n = 2$ modes for the isovector- and isoscalar-like volume particle density vibrations, respectively (solid lines in Figs. 3 and 4 for the zero L and dotted and dashed lines for the finite L) has a somewhat remarkable shape asymmetry [31, 36]. For SLy5* (Fig. 3) and for SVsym32 (Fig. 4) one has the "in-phase" satellite to the right of the main "out-of-phase" peak, cf. with the traditional PDR to the left of the main one. An enhancement to the left

of the main peak for SLy5* is from increasing the "out-of-phase" strength (red solid and magenta rare dotted curves, Fig. 3) at small energies because of the appearance of a peak at the energy about a few MeV, in contrast to the SVsym32 case. The semiclassical FLD model calculations at the lowest $\hbar$ order should be improved here, for instance by taking into account the quantum effects like shell corrections within more general periodic-orbit theory [51, 52]. In the nucleus ^{132}Sn the IVDR energies of the two peaks do not change much with L in both cases: $E_1 = 17$ MeV, $E_2 = 20$ MeV for SLy5* (Fig. 3) and $E_1 = 15$ MeV, $E_2 = 18$ MeV for SVsym32 (Fig. 4). We find only an essential re-distribution of the EWSR contributions (normalized to 100% for the EWSR sum of the main and satellite peaks) [Eq. (41) for $S_n^{(1)}$]. This is from a significant enhancement of the main "out-of-phase" peak with increasing L, $S_1^{(1)} = 89\%$ and $S_2^{(1)} = 11\%$ for SLy5* (Fig. 3) and more pronounced EWSR distribution $S_1^{(1)} = 76\%$ and $S_2^{(1)} = 24\%$ for SVsym32 (Fig. 4) [cf. with the corresponding $L = 0$ results: $S_1^{(1)} = 88\%$ and $S_2^{(1)} = 12\%$ for SLy5* and $S_1^{(1)} = 73\%$ and $S_2^{(1)} = 27\%$ for SVsym32].

Figures 5 and 6 show more systematic study for several isotopes and for the chain of the Sn isotopes, respectively. In Fig. 6, we compare the results of our calculations with the experimental data. The latter were obtained by fitting the experimental strength curve for a given almost spherical Sn isotope by the two Lorenzian oscillator strength functions as described in Refs. [30, 51]. It is always possible in the case of the asymmetric shapes of the strength curves with usual enhancement on the right of the main peak, even in the case when the satellite cannot be distiguished transparently well from the main peak in almost spherical nuclei (unlike the clear shoulders for the IVDRs in deformed ones). Each of these functions has three fitting parameters such as the inertia, stiffness and width of the peak. We found somewhat good agreement of our ETF ES results with these experimental data for the energies, ratio of the strengths at the satellite to the main modes, and the EWSR contributions.

More precise L-dependent calculations change essentially the IVDR strength distribution for the SV forces because of the smaller $c_{\rm sym}$ value as compared to other Skyrme interactions (see Table I). For ^{208}Pb one obtains $E_1 = 15$ MeV, $S_1^{(1)} = 91\%$ for the main peak and $E_2 = 17$ MeV, $S_2^{(1)} = 9\%$ the satellite for SLy5*; and $E_1 = 13$ MeV, $S_1^{(1)} = 83\%$ for the main peak and $E_2 = 16$ MeV, $S_2^{(1)} = 17\%$ the satellite for SVsym32 forces. These calculations are qualitatively in agreement with the experimental results: $E_1 = 13$ MeV, $S_1^{(1)} = 98\%$ for the main peak and $E_2 = 17$ MeV, $S_2^{(1)} = 2\%$ the satellite. Discrepancies might be related to the strong shell effects in this stable double magic nucleus which are neglected in the ETF ES approach.

Decreasing the relaxation time $\mathcal{T}$ by a factor of about 1.5 almost does not change the IVDR strength structure. However, we found a strong dependence on the relaxation time $\mathcal{T}$ in a wider region of $\mathcal{T}$ values. The "in-phase" strength component with a wide maximum does not depend much on the Skyrme force [37, 41, 43], the slope parameter L, and the relaxation time $\mathcal{T}$. We found also a regular change of the IVDR strength for different double magic isotopes (Fig. 5). In addition to a big change for the energy (mainly because of E_1) and the strength $[S_1(\omega)]$, one also obtains more asymmetry for ^{68}Ni than for the other isotopes. Calculations for nuclei with different mass A were performed with the relaxation time $\mathcal{T}$ [Eq. (39)] where $\mathcal{T}_0 = \mathcal{T}_{0\rm Pb}(208/A)^{1/3}$ with the parameter $\mathcal{T}_{0\rm Pb} = 300$ MeV$^2\cdot$s derived from the IVGDR width of ^{208}Pb, in agreement with experimental data for the averaged A dependence of the IVGDR widths ($\propto A^{-2/3}$). In this way the IVDR relaxation time $\mathcal{T}_n$ becomes larger with increasing A as $A^{1/3}$, and at the same time, the height of peaks decreases. The L corrections are also changing much in the same scale of all three nuclei.

The essential parameter of the Skyrme HF approach leading to the significant differences in the k_S and Q values is the constant $\mathcal{C}_-$ [Eq. (2) and Table I]. Indeed, $\mathcal{C}_-$ is the key quantity in the expression for Q [Eq. (27)] and the isovector surface-energy constant k_S [or $b_S^{(-)}$, Eq. (21)], because $Q \propto 1/k_S \propto 1/\mathcal{C}_-$ and $k_S \propto \mathcal{C}_-$ [7]. Concerning k_S and the IVDR strength structure, this is even more important than the L dependence although the latter changes significantly the isovector stiffness Q and the neutron skin τ. As seen in Table I, the constant $\mathcal{C}_-$ is very different in absolute value and in sign for different Skyrme forces whereas $\mathcal{C}_+$ is almost constant (Table I). The isoscalar energy density constant $b_S^{(+)}$ is proportional to C_+ [Eq. (20)], in contrast to the isovector one. All Skyrme parameters are fitted to the well-known experimental value $b_S^{(+)} = 17 - 19$ MeV while there are so far no clear experiments which would determine k_S well enough because the mean energies of the IVGDR (main peaks) do not depend very much on k_S for different Skyrme forces (the last three rows of Table II). Perhaps, the low-lying isovector collective states are more sensitive but at the present time there is no careful systematic study of their k_S dependence. Another reason for so different k_S and Q values might be because of difficulties in deducing k_S directly from the HF calculations because of the curvature and quantum effects. In this respect, the semi-infinite Fermi system with a hard plane wall might be more adequate for the comparison of the HF theory and the ETF effective surface approach. We have also to go far away from the nuclear stability line to subtract uniquely the coefficient k_S in the dependence of $b_S^{(-)} \propto I^2 = (N-Z)^2/A^2$, according to Eq. (21). For exotic nuclei one has more problems to derive k_S from the experimental data with enough precision. Note that, for studying the IVDR structure, the quantity k_S is more fundamental than the isovector stiffness Q because of the direct relation to the tension coefficient σ_- of the isovector capillary pressure. Therefore, it is simpler to analyze

the experimental data for the IVGDR within the macroscopic HD or FLD models in terms of the constant k_S. The quantity Q involves also the ES approximation for the description of the nuclear edge through the neutron skin τ in Eq. (24). The L dependence of the neutron skin τ is essential but not so dramatic in the case of SLy and SV forces (Table II), except for the SVmas08 forces with the effective mass 0.8. The precision of such a description depends more on the specific nuclear models [19, 20, 27]. On the other hand, the neutron skin thickness τ, like the stiffness Q, is interesting in many aspects for an investigation of exotic nuclei, in particular, in nuclear astrophysics.

We emphasize that for specific Skyrme forces there exists an abnormal behavior of the isovector surface constants k_S and Q. It is related to the fundamental constant $\mathcal{C}_-$ of the energy density (2) but not to the derivative symmetry-energy density corrections. For the parameter set T6 ($\mathcal{C}_- = 0$) one finds $k_S = 0$ (Ref. [7]). Therefore, according to Eq. (27), the value of Q diverges (ν is almost independent from $\mathcal{C}_-$ for SLy and SV forces; Table II and Refs. [7, 31, 36]). The isovector gradient terms which are important for the consistent derivations within the ES approach are also not included ($\mathcal{C}_- = 0$) into the symmetry energy density in Refs. [15, 17, 18]. In relativistic investigations [12, 13] of the structure of the IVGR distributions, the dependence of these quantities on the derivative terms has not been investigated so far. It therefore remains an interesting task for the future to apply similar semiclassical methods such as the ES approximation used here also in relativistic models. Moreover, for RATP [37] and SV [41] (like for SkI) Skyrme forces, the isovector stiffness Q is even negative as $\mathcal{C}_- > 0$ ($k_S > 0$) in contrast to other Skyrme forces. This would lead to an instability of the vibration of the neutron skin.

Table II shows also the coefficients ν of Eq. (27) for the isovector stiffness Q. They are almost constant for all SLy and SV Skyrme forces, in contrast to other forces [7]. However, these constants ν, being sensitive to the SO (β) dependence through Eqs. (26), (25) and (22), change also with L (Table II). As compared to 9/4 suggested in Ref. [8], they are significantly smaller in magnitude for most of the Skyrme forces.

In Fig. 7 we show, in the case of the Skyrme forces SLy5* and SVsym32, the transition densities $\rho^{\omega}_{\mp}(x)$ of Eq. (33) for the "out-"of-phase (-) and the "in-"phase (+) modes of the volume vibrations at the excitation energy E_2 of the satellite. The transition densities were not presented in our preliminary publication [36]. These are the key quantities for the calculation of the IVDR strengths, according to Eq. (32). The L dependence is somewhat small, slightly notable mostly near the ES ($|x| \lesssim 1$). From Fig. 8, one finds a remarkable neutron vs proton excess near the nuclear edge for the same forces, which is however, very slightly depending on the slope parameter L. A small dependence of the transition densities on L comes through the symmetry-energy constant k_S which is almost the same in modulus for these forces. We did not find a dramatic change of the transition densities with the sign of k_S. Therefore, there is a weak sensitivity of the transition densities on L through the energy E_2. We would have expected a stronger influence of the sign of k_S on the vibrations of the neutron skin rather than on the IVDR. This different sign leads to the opposite, stable and unstable, neutron skin vibrations. One observes also other differences between the upper (SLy5*) and the lower (SVsym32) panels in both figures: We find a redistribution of the surface-to-volume contributions of the transition densities for these two modes. Again, as in Figs. 9 and 10, one finds a considerable change of the neutron-proton transition densities for the different isotopes for SLy5* and SVsym32.

The last figure shows theoretical (Fig. 11) evaluations of the neutron skin. Figure 11 shows the absolute values of the skin obtained from τ/I multiplying the mean-square evaluations of the nuclear radii by the factor $\sqrt{3/5}$ for an easy comparison with experimental data given in [27]. For ^{208}Pb, one finds that the experimental values $\Delta r_{np}^{exp} = 0.12 - 0.14$ fm in Ref. [27] ($0.156^{+0.025}_{-0.021}$ fm [59]) are in good agreement with our calculations $\Delta r_{np}^{theor} \approx 0.10 - 0.13$ fm within the ES approximation (the limits show values from SLy5* to SVsym32). For the isotope ^{124}Sn one obtains $\Delta r_{np}^{theor} \approx 0.09 - 0.12$ fm, also in good agreement with experimental results. For the isotope ^{132}Sn, we predict the value $\Delta r_{np}^{theor} \approx 0.11 - 0.15$ fm. Similarly, for ^{60}Ni and ^{68}Ni, one finds $\Delta r_{np}^{theor} \approx 0.03 - 0.04$ (like in Ref. [27]) and $0.08 - 0.11$ fm, respectively.

VIII. CONCLUSIONS

The slope parameter L was taken into account in the leading ES approximation to derive simple analytical expressions for the isovector particle densities and energies. These expressions were used for calculations of the surface symmetry energy, the neutron skin thickness, and the isovector stiffness coefficients as functions of L. For the derivation of the surface symmetry energy and its dependence on the particle density we have to include main higher order terms in the parameter a/R. These terms depend on the well-known parameters of the Skyrme forces. Results for the isovector surface-energy constant k_S, the neutron skin thickness τ and the stiffness Q depend in a sensitive way on the parameters of the Skyrme functional (especially on the parameter $\mathcal{C}_-$) in the gradient terms of the density in the surface symmetry energy [see Eq. (2)]. The isovector constants k_S, τ and Q depend also essentially on the slope parameter L, in addition to the SO interaction constant β. For all Skyrme forces, the isovector stiffness constants Q are significantly larger than those obtained in earlier investigations. However, taking into account their L-dependence they come closer to the empirical data. It influences more on the isovector stiffness Q and on the neutron skin τ, than on the surface symmetry-energy constant k_S. The mean IVGDR ener-

gies and sum rules calculated in the macroscopic models like the FLD model [6, 30] in Table II are in fairly good agreement with the experimental data for most of the k_S values. As compared with the experimental data and other recent theoretical works, we found a somewhat reasonable two-peak structure of the IVDR strength within the FLD model. According to our results for the neutron and proton transition densities [Figs. 8-10], we may interpret semiclassically the IVDR satellites as some kind of pygmy resonances, in addition to the traditional studies [12–14, 22–25, 32–35]. Their energies, sum rules and n-p transition densities obtained analytically within the semiclassical FLD approximation are sensitive to the surface symmetry-energy constant k_s and the slope parameter L. Therefore, their comparison with the experimental data can be used for the evaluation of k_s and L. It seems helpful to describe them in terms of only few critical parameters, like k_S and L.

For further perspectives, it would be worthwhile to apply our results to calculations of the IVDR strength structure within the FLD model [30] in a more systematic way. In this respect it is also interesting that the low-lying collective isovector states are expected to be even more sensitive to the values of k_S within the periodic orbit theory [52, 60, 61]. More general problems of classical and quantum chaos in terms of the level statistics and Poincare and Lyapunov exponents (Ref. [62] and references therein) might lead to progress in studying the fundamental properties of collective dynamics like nuclear fission within the Swiatecki-Strutinsky macroscopic-microscopic model. Our approach is helpful also for further study of the effects in the surface symmetry energy because it gives analytical universal expressions for the constants k_S, τ and Q as functions of the slope parameter L which do not depend on specific properties of nuclei as they are directly connected with a few critical parameters of the Skyrme interaction without any fitting.

Acknowledgements

The authors thank V.I. Abrosimov, K. Arita, V.Yu. Denisov, V.M. Kolomietz, M. Kowal, M. Matsuo, K. Matsuyanagi, J. Meyer, V.O. Nesterenko, M. Pearson, V.A. Plujko, P.-G. Reinhard, A.I. Sanzhur, J. Skalski, and X. Vinas for many useful discussions. One of us (A.G.M.) is also very grateful for the warm hospitality during working visits at the National Centre for Nuclear Research in Warsaw, Poland, and also for financial support from the Japanese Society of Promotion of Sciences, Grant No. S-14130, during his stay at the Nagoya Institute of Technology. This work was partially supported by the Deutsche Forschungsgemeinschaft Cluster of Excellence Origin and Structure of the Universe (www.universe-cluster.de).

Appendix A: SOLUTIONS OF THE ISOVECTOR LAGRANGE EQUATION

The Lagrange equation for the variations of the isovector particle density ρ_- is given in the local coordinates ξ, η by [5, 7]

$$2\mathcal{C}_-\frac{\partial^2\rho_-}{\partial\xi^2} + 2\mathcal{C}_-\mathcal{H}\frac{\partial\rho_-}{\partial\xi} - \frac{\mathrm{d}}{\mathrm{d}\rho_-}\left[\rho_+\varepsilon_-\left(\rho_+,\rho_-\right)\right] + \lambda_- = 0, \tag{A1}$$

where $\mathcal{H}$ is the mean curvature of the ES, λ_- is the ES correction to the isovector chemical potential. Up to the leading terms in a small parameter a/R one gets from Eq. (A1)

$$2\mathcal{C}_-\,\frac{\partial^2\rho_-}{\partial\xi^2} - \frac{\mathrm{d}}{\mathrm{d}\rho_-}\left[\rho_+\varepsilon_-(\rho_+,\rho_-)\right] = 0\ . \tag{A2}$$

We neglected here the higher order terms proportional to the first derivatives of the particle density ρ_- with respect to ξ and the surface correction to the isovector chemical potential in Eq. (A1) (Refs. [2, 3] for the isoscalar case). For the dimensionless isovector density $w_- = \rho_-/(\overline{\rho}I)$ one finds after simple transformations the following equation and the boundary condition in the form

$$\frac{\mathrm{d}w_-}{\mathrm{d}w} = c_{\rm sym}\sqrt{\frac{\overline{\mathcal{S}}_{\rm sym}(\epsilon)(1+\beta w)}{e[\epsilon(w)]}}\sqrt{\left|1-\frac{w_-^2}{w^2}\right|}, \quad w_-(w=1) = 1\ , \tag{A3}$$

where β is the SO parameter defined below Eq. (9), $\overline{\mathcal{S}}_{\rm sym} = \mathcal{S}_{\rm sym}/J$, $c_{\rm sym}$ is defined in Eq. (12) and $\mathcal{S}_{\rm sym}(\epsilon)$ in Eq. (6). The above equation determines the isovector density w_- as a function of the isoscalar one $w(x)$ [Eq. (9)]. In the quadratic approximation for $e[\epsilon(w)]$ [up to a small asymmetry correction proportional to I^2 in Eq. (4)], one finds an explicit analytical expression in terms of elementary functions [7]. Substituting $w_- = w\,\cos\psi$ into Eq. (A3), and taking the approximation $e = (1-w)^2$, one has the following first order differential equation for a new function $\psi(w)$:

$$-\frac{w(1-w)}{c_{\rm sym}}\,\sin\psi\,\frac{\mathrm{d}\psi}{\mathrm{d}w} = \sqrt{\overline{\mathcal{S}}_{\rm sym}(\epsilon)(1+\beta w)}\,\sin\psi - \frac{1-w}{c_{\rm sym}}\,\cos\psi, \qquad \psi(w=1) = 0. \tag{A4}$$

The boundary condition for this equation is related to that of Eq. (A3) for $w_-(w)$. This equation looks more complicated because of the trigonometric nonlinear terms. However, it allows one to obtain simple approximate analytical solutions within standard perturbation theory. Indeed, according to Eqs. (A3) and (9), where we do not have an explicit x-dependence, we note that w_- is mainly a sharply decreasing function of x through $w(x)$ within a small diffuseness region of the order of one in dimensionless units (Figs. 1 and 2). Thus, we may find approximate solutions to Eq. (A4) with its boundary condition in terms of a power expansion of a new

function $\widetilde{\psi}(\gamma)$ in terms of a new small argument γ [Eq. (12)]

$$\widetilde{\psi}(\gamma) \equiv \psi(w) = \sum_{n=0}^{\infty} c_n\, \gamma^n(w)\,, \tag{A5}$$

where the coefficients c_n and γ are defined in Eq. (12). Substituting the power series (A5) into Eq. (A4), one expands first the trigonometric functions into a power series of γ according to the boundary condition in Eq. (A4). As usual, using standard perturbation theory, we obtain a system of algebraic equations for the coefficients c_n [Eq. (A5)] by equating coefficients from both sides of Eq. (A4) with the same powers of γ. This simple procedure leads to a system of algebraic recurrence relations which determine the coefficients c_n as functions of the parameters β and $c_{\rm sym}$ of Eq. (A4),

$$c_0 = 0, \qquad c_1 = \frac{1}{\sqrt{1+\beta}}, \tag{A6}$$

$$c_2 = \frac{c_1}{2c_{\rm sym}(1+\beta)}\left(\beta c_{\rm sym}^2 + 2 + \frac{L}{3J}c_{\rm sym}^2(1+\beta)\right),$$

$$c_3 = -c_1\left\{\frac{4}{3}c_1^2 - 3\frac{c_1c_2}{c_{\rm sym}} - \frac{c_2c_{\rm sym}}{2c_1}\left(\beta c_1^2 + \frac{L}{3J}\right)\right.$$

$$\left. - \frac{1}{8}\beta^2 c_{\rm sym}^2 c_1^4 + \frac{K_- c_{\rm sym}^2}{36J} + \frac{c_{\rm sym}^2 L}{12J}\left(\beta c_1^2 - \frac{L}{6J}\right)\right\},$$

and so on. In particular, up to second order in γ, we derive analytical solutions as functions of β, $c_{\rm sym}$, J and L in an explicitly closed form:

$$\widetilde{\psi}(\gamma) = \gamma\,(c_1 + c_2\gamma)\,, \qquad c_1 = \frac{1}{\sqrt{1+\beta}}, \tag{A7}$$

$$c_2 = \frac{\beta c_{\rm sym}^2 + 2 + Lc_{\rm sym}^2(1+\beta)/(3J)}{2(1+\beta)^{3/2}c_{\rm sym}}. \tag{A8}$$

Thus, using the standard perturbation expansion method of solving $\widetilde{\psi}(\gamma)$ in terms of the power series of the γ up to γ^2, one obtains the quadratic expansion of $\psi(w)$ [Eq. (13)] with $\widetilde{c} = c_2/c_1$. Notice that one finds a good convergence of the power expansion of $\widetilde{\psi}(\gamma(w))$ (A7) in $\gamma(w)$ for $w_-(x)$ at the second order in $\gamma(w)$ because of values of $c_{\rm sym}$ larger one for all Skyrme forces presented in Table I [Eq. (12) for $c_{\rm sym}$].

Appendix B: Derivations of the surface energy and its coefficients

For the calculation of the surface energy components $E_S^{(\pm)}$ of the energy E in Eq. (1) within the same improved ES approximation as described above in Appendix A we first separate the volume terms related to the first two terms of Eq. (2) for the energy density $\mathcal{E}$ per particle. Other terms of the energy density $\rho\mathcal{E}(\rho_+,\rho_-)$ in Eq. (2) lead to the surface components $E_S^{\pm}$ [Eq. (18)], as they are concentrated near the ES. Integrating the energy density $\rho\mathcal{E}$ per unit of the volume [see Eq. (2)] over the spatial coordinates $\mathbf{r}$ in the local coordinate system ξ,η (see Fig. 1) in the ES approximation, one finds

$$E_S^{\pm} = \oint \mathrm{d}S \int_{\xi_{in}}^{\infty} \mathrm{d}\xi \left[\mathcal{C}_\pm\left(\nabla\rho_\pm\right)^2 + \rho_+\varepsilon_\pm\left(\rho_+,\rho_-\right)\right]$$

$$\approx \sigma_\pm\, S, \tag{B1}$$

where $\xi_{in} \lesssim -a$ (Refs. [2, 3, 5]). The local coordinates ξ,η were used because the integral over ξ converges rapidly within the ES layer which is effectively taken for $|\xi| \lesssim a$. Therefore again, we may extend formally ξ_{in} to $-\infty$ in the first (internal) integral taken over the ES in the normal direction ξ in Eq. (B1). Then, the second integration is performed over the closed surface of the ES. The integrand over ξ contains terms of the order of $(\overline{\rho}/a)^2 \propto (R/a)^2$ like the ones of the leading order in the first equation of Ref. [7]. However, the integration is effectively performed over the edge region of the order of a that leads to the additional smallness proportional to a/R like in Appendix A. At this leading order the η dependence of the internal integrand can be neglected. Moreover, from the Lagrange equations [see Eq. (A2) for the isovector case] at this order one can realize that terms without the particle density gradients in Eq. (B1) are equivalent to the gradient terms. Therefore, for the calculation of the internal integral we may approximately reduce the integrand over ξ to derivatives of the universal particle densities of the leading order $\rho_\pm(\xi)$ in ξ using $\mathcal{C}_\pm\left(\nabla\rho_\pm\right)^2 + \rho_+\varepsilon_\pm\left(\rho_+,\rho_-\right) \approx 2\mathcal{C}_\pm(\partial\rho_\pm/\partial\xi)^2$ [see Eqs. (9) and (13) for $w_\pm(x)$] . We emphasize that the isovector gradient terms are obviously important for these calculations. Taking the integral over ξ within the infinite integration region $(-\infty < \xi < \infty)$ out of the integral over the ES ($\mathrm{d}S$) we are left with the integral over the ES itself that is the surface area $\mathcal{S}$. Thus, we arrive finally at the right-hand side of Eq. (B1) with the surface tension coefficient $\sigma_\pm = b_S^{(\pm)}/(4\pi r_0^2)$ [see Eq. (19) for $b_S^{(\pm)}$].

Using now the quadratic approximation $e[\epsilon(w)] = (1-w)^2$ in Eq. (19) for $b_S^{\pm}$ ($\mathcal{D}_- = 0$) one obtains (for $\beta < 0$, see Table I)

$$b_S^{(\pm)} = 6\overline{\rho}\,\mathcal{C}_\pm\,\frac{\mathcal{J}_\pm}{r_0 a}\,, \tag{B2}$$

where

$$\mathcal{J}_+ = \int_0^1 \mathrm{d}w\,\sqrt{w(1+\beta w)}\,(1-w) \tag{B3}$$

$$= \frac{1}{24(-\beta)^{5/2}} \times$$

$$\times\left[\mathcal{J}_+^{(1)}\,\sqrt{-\beta(1+\beta)} + \mathcal{J}_+^{(2)}\,\arcsin\sqrt{-\beta}\right],$$

with

$$\mathcal{J}_+^{(1)} = 3 + 4\beta(1+\beta), \qquad \mathcal{J}_+^{(2)} = -3 - 6\beta\,. \tag{B4}$$

For the isovector energy constant $\mathcal{J}_-$ one finds

$$\mathcal{J}_- = \frac{-1}{1+\beta}\int_0^1 \mathrm{d}w\,\sqrt{w(1+\beta w)}(1-w)(1+\widetilde{c}\gamma(w))^2$$
$$= \frac{\widetilde{c}^2}{1920(1+\beta)(-\beta)^{9/2}}\left[\mathcal{J}_-^{(1)}\left(\frac{c_{\rm sym}}{\widetilde{c}}\right)\sqrt{-\beta(1+\beta)}\right.$$
$$\left. + \mathcal{J}_-^{(2)}\left(\frac{c_{\rm sym}}{\widetilde{c}}\right)\arcsin\sqrt{-\beta}\right], \quad \text{(B5)}$$

with

$$\mathcal{J}_-^{(1)}(\zeta) = 105 - 4\beta\left\{95+75\zeta+\beta\left[119+10\zeta(19+6\zeta)\right.\right.$$
$$\left.\left. + 8\beta^2(1+10\zeta(1+\zeta)) + 8\zeta(5\zeta(3+2\zeta)-6)\right]\right\},$$
$$\mathcal{J}_-^{(2)}(\zeta) = 15\left\{7+2\beta\left[5(3+2\zeta)+8\beta(1+\zeta)\right.\right.$$
$$\left.\left. \times\ (3+\zeta+2\beta(1+\zeta))\right]\right\}. \quad \text{(B6)}$$

These equations determine explicitly the analytical expressions for the isoscalar ($b_S^{(+)}$) and isovector ($b_S^{(-)}$) energy constants in terms of the Skyrme force parameters; see Eq. (15) for $\widetilde{c}$ and Eq. (12) for $c_{\rm sym}$ and $\gamma(w)$. For the limit $\beta \to 0$ one has from Eqs. (B3) and (B5) $\mathcal{J}_\pm \to 4/15$. With Eqs. (25) and (26) one arrives also at the explicit analytical expression for the isovector stiffness Q as a function of $\mathcal{C}_-$ and β. In the limit $\mathcal{C}_- \to 0$ one obtains $k_S \to 0$ and $Q \to \infty$ because of the finite limit of the argument $c_{\rm sym}/\widetilde{c} \to 2(1+\beta)/[\beta+(1+\beta)L/(3J)]$ of the function $\mathcal{J}_-$ in Eq. (B5) [see also Eqs. (13) for $\widetilde{c}$ and Eq. (12) for $c_{\rm sym}$].

[1] V.M. Strutinsky and A. S. Tyapin, JETP (Soviet Phys.) **18**, 664 (1964).
[2] V.M. Strutinsky, A.G. Magner, and M. Brack, Z. Phys. A **319**, 205 (1984).
[3] V.M. Strutinsky, A.G. Magner, and V. Yu. Denisov, Z. Phys. A **322**, 149 (1985).
[4] M. Brack, C. Guet, and H.-B. Hakansson, Phys. Rep. **123**, 275 (1985).
[5] A.G. Magner, A.I. Sanzhur, and A.M. Gzhebinsky, Int. J. Mod. Phys. E **18**, 885 (2009).
[6] J.P. Blocki, A.G. Magner, and A.A. Vlasenko, Nucl. Phys. and At. Energy, **13**, 333 (2012).
[7] J.P. Blocki, A.G. Magner, P.Ring, and A.A. Vlasenko, Phys.Rev. C **87**, 044304 (2013).
[8] W.D. Myers and W.J. Swiatecki, Ann. Phys. (NY) **55**, 395 (1969); W.D. Myers and W.J. Swiatecki, Ann. Phys. (NY) **84**, 186 (1974).
[9] W.D. Myers, W.J. Swiatecki, Nucl.Phys. A **336**, 267 (1980); W.D. Myers, W.J. Swiatecki, Nucl.Phys. A **601**, 141 (1996).
[10] W.D. Myers et al., Phys. Rev. C **15**, 2032 (1977).
[11] W.D. Myers, W.J. Swiatecki, and C.S. Wang, Nucl.Phys. A **436**, 185 (1985).
[12] D. Vretenar, N. Paar, P. Ring and G. A. Lalazissis, Phys. Rev. C **63**, 047301 (2001).
[13] D. Vretenar, N. Paar, P. Ring and G.A Lalazissis, Nucl. Phys. A **692**, 496 (2001).
[14] N. Ryezayeva, T. Hartmann, Y. Kalmykov et al., Phys. Rev. Lett., **89**, 272502 (2002).
[15] P. Danielewicz, Nucl. Phys. A **727**, 233 (2003).
[16] M. Samyn, S. Goriely, M. Bender, and J.M. Pearson, Phys. Rev. C, **70**, 044309 (2004).
[17] P. Danielewicz and J. Lee, Int. J. Mod. Phys. E **18**, 892 (2009).
[18] P. Danielewicz, Nucl.Phys. A **818**, 36 (2009).
[19] M. Centelles, X. Roca-Maza, X. Vinas, and M. Warda, Phys. Rev. Lett., **102**, 122502 (2009).
[20] M. Warda, X. Vinas, X. Roca-Maza, and M. Centelles, Phys. Rev. C **80**, 024316 (2009); M. Warda, X. Vinas, X. Roca-Maza, and M. Centelles, Phys. Rev. C **81**, 054309 (2010); M. Warda, X. Vinas, X. Roca-Maza, and M. Centelles, Phys. Rev. C **82**, 054314 (2010).
[21] X. Roca-Maza, M. Centelles, X. Vinas, and M. Warda, Phys. Rev. Lett. **106**, 252501 (2011).
[22] A. Voinov et al., Phys. Rev. C **81** 024319 (2010). (2010).
[23] A.C. Larsen et al., Phys. Rev. C **87**, 014319 (2013).
[24] A. Repko, P.-G. Reinhard, V.O. Nesterenko, and J. Kvasil, Phys. Rev. C **87**, 024305 (2013).
[25] W. Kleinig, V. O. Nesterenko, J. Kvasil, P.-G. Reinhard, and P. Vesely, Phys. Rev. C **78**, 044313 (2008).
[26] J. Kvasil, A. Repko, V.O. Nesterenko, W. Kleining, P.-G. Reinhard, Phys. Scr. T **154**, 014019 (2013).
[27] X. Vinas, M. Centelles, X. Roca-Maza, and M. Warda, Eur. Phys. J. A **50**, 27 (2014).
[28] J. Endres et al., Phys. Rev. Lett. **105**, 212503 (2010).
[29] V.M. Kolomietz and A.G. Magner, Phys. Atom. Nucl. **63**, 1732 (2000).
[30] V.M. Kolomietz, A.G. Magner, and S. Shlomo, Phys. Rev. C **73**, 024312 (2006).
[31] J.P. Blocki, A.G. Magner, and P. Ring, Phys. Scr. T**89**, 054019 (2014).
[32] P. Adrich et al., Phys. Rev. Lett., **95**, 132501 (2005).
[33] N. Paar, D. Vretenar, E. Khan, and G. Colo, Rep. Prog. Phys. **70**, 691 (2007).
[34] O. Wieland et al., Phys. Rev. Lett., **102**, 092502 (2009).
[35] D. Savran, T. Aumann, and A. Zilges, Prog. Part. Nucl. Phys. **70**, 210 (2013).
[36] J.P. Blocki, A.G. Magner, and P. Ring, Phys. Scr. T **90**, 114009 (2015).
[37] E. Chabanat et al., Nucl. Phys. A **627**, 710 (1997); E. Chabanat et al., Nucl. Phys. A **635**, 231 (1998).
[38] P.-G. Reinhard and H. Flocard, Nucl. Phys. A **585**, 467 (1995).
[39] M. Bender, P.-H. Heenen, P.-G. Reinhard, Rev. Mod. Phys. **75**, 125 (2003).
[40] J.R. Stone and P.-G. Reinhard, Prog. Part. Nucl. Phys.

58, 587 (2007).
[41] P. Klüpfel P, P.-G. Reinhard, T.J. Bürvenich, and J.A. Maruhn, Phys. Rev. C **79**, 034310 (2009).
[42] J. Erler, C.J. Horowitz, W. Nazarevich, M. Rafalski, and P.-G. Reinhard, arXiv:1211.6292v1 [nucl-th] (2012).
[43] A. Pastore et al., Phys. Scr. T **154**, 014014 (2013).
[44] J. Meyer (private communications, 2014).
[45] B.-A. Li, L.-W. Chen, C.M. Ko, Phys. Rep. **464**, 113 (2008).
[46] H. Q. Gu, H. Z. Liang, W. H. Long, N. V. Giai, and J. Meng, Phys. Rev. C **87**, 041301 (2013).
[47] Aa. Bohr and B. Mottelson, *Nuclear Structure*, Vol. II (W.A. Benjamin, New York, 1975).
[48] A.G. Magner and V.M. Strutinsky, Z. Phys. A **322**, 633 (1985).
[49] A.G. Magner, Sov. J. Nucl. Phys. **45**, 235 (1987) [Yad. Fiz. **45**, 374 (1987)].
[50] V. Yu. Denisov, Sov. J. Nucl. Phys. **43**, 28 (1986).
[51] A.G. Magner, D.V. Gorpinchenko, and J. Bartel, Phys. Atom. Nucl., **77**, 1229 (2014).
[52] J.P. Blocki and A.G. Magner, Phys. Scr. T **154**, 014006 (2013).
[53] J.M. Eisenberg, W. Greiner, *Nuclear Theory, Vol. I, Nuclear Models Collective and Single-Particle Phenomena* (North-Holland, Amsterdam/London, 1970).
[54] B.L. Berman and S.C. Fulz, Rev. Mod. Phys. **47**, 713 (1975).
[55] A. Van der Woude, Prog. Part. Nucl. Phys. **18**, 217 (1987).
[56] V.V. Varlamov, V.V. Sapunenko, and M.E. Stepanov, in *Photonuclear Data 1976-1995* (Moscow State University, Moscow, 1996), pp. 1–220 [http://cdfe.sinp.msu.ru/service/index.html].
[57] V.V. Varlamov, B.S. Ishanov, and M.E. Stepanov, *Systematics of Main Parameters of Atomic Nuclei Giant Dipole Resonances and Photonuclear Reaction Threshold Values* (Moscow State University, Institute of Nuclear Physics, Moscow, 1996).
[58] S.S. Dietrich and B.L. Berman, At. Data Nucl. Data Tables **38**, 199 (1988).
[59] A. Tamii et. al., Phys. Rev. Lett. **107**, 062502 (2011).
[60] A.M. Gzhebinsky, A.G. Magner, and S.N. Fedotkin, Phys. Rev. C **76**, 064315 (2007).
[61] J.P. Blocki, A.G. Magner, and I.S. Yatsyshyn, Int. J. Mod. Phys. E **21**, 1250034 (2012).
[62] J.P. Blocki and A.G. Magner, Phys. Rev. C **85**, 064311 (2012).

	SkM*	SGII	SLy5	SLy5*	SLy6	SLy7	SVsym28	SVsym32	SVmas08	SVK226	SVkap02
$\overline{\rho}$ (fm^{-3})	0.16	0.16	0.16	0.16	0.17	0.16	0.16	0.16	0.16	0.16	0.16
b_V (MeV)	15.8	15.6	16.0	16.0	17.0	15.9	15.9	15.9	15.9	15.9	15.9
K (MeV)	217	215	230	230	245	230	234	234	234	226	234
J (MeV)	30.0	26.8	32.0	32.0	32.0	32.0	28.0	32.0	30.0	30.0	30.0
L (MeV)	47.5	37.7	48.3	45.9	47.4	47.2	7.5	59.5	42.0	35.5	37.0
$\mathcal{C}_+$ (MeV·fm^5)	57.6	43.9	59.3	60.1	54.1	52.7	49.6	51.8	50.9	51.4	50.7
$\mathcal{C}_-$ (MeV·fm^5)	-4.79	-0.94	-22.8	-24.2	-15.6	-13.4	19.6	26.0	36.9	30.6	21.9
$c_{\rm sym}$	3.24	6.07	1.58	1.54	1.77	1.95	1.48	1.40	1.13	1.22	1.46
β	-0.64	-0.54	-0.58	-0.52	-0.62	-0.65	-0.48	-0.47	-0.51	-0.48	-0.48

TABLE I. Basic parameters of some critical Skyrme forces from Refs. [37, 41], including the L derivatives [20, 41, 44]. In addition to these standard quantities, are the isoscalar and isovector constants $C_\pm$ of the energy density gradient terms [Eqs. (2) and (8)]; $c_{\rm sym}$ is given by Eq. (12) and the spin-orbit constant β is defined below Eq. (9).

	SkM*	SGII	SLy5	SLy5*	SLy6	SLy7	SVsym28	SVsym32	SVmas08	SVK226	SVkap02
$k_{S,0}$(MeV)	-2.47	-0.53	-12.6	-13.1	-9.03	-7.09	11.4	15.6	37.1	23.7	12.7
k_S(MeV)	-2.48	-0.46	-14.6	-15.0	-10.1	-7.61	13.3	18.2	46.7	29.5	14.8
ν_0	163	21.9	0.59	0.92	1.21	1.99	0.90	0.84	0.89	0.79	0.89
ν	2.27	1.89	0.28	0.60	0.62	0.73	0.58	0.61	0.86	0.70	0.59
Q_0(MeV)	59642	29908	73	72	137	287	-62	-55	-62	-30	-63
Q(MeV)	823	2570	42	41	63	98	-34	-34	-34	-21	-36
τ_0/I	0.006	0.004	0.41	0.43	0.26	0.16	0.43	0.53	0.040	0.89	0.45
τ/I	0.055	0.014	0.59	0.60	0.40	0.28	0.62	0.73	1.68	1.18	0.64
D_0(MeV) ^{132}Sn	89	91	101	89	104	102	78	79	81	77	84
D(MeV) ^{68}Ni	91	92	100	88	104	95	79	80	83	78	85
^{132}Sn	89	91	100	89	103	95	77	78	81	76	83
^{208}Pb	90	91	109	88	102	93	77	78	81	76	82

TABLE II. The isovector energy k_S and the stiffness Q coefficients are shown for several Skyrme forces [37, 41, 44]; ν is the constant of Eq. (27); τ/I is the neutron skin thickness calculated by Eq. (25) with the corresponding L ; the functions $D(A)$ for the FLD model in the last three lines are calculated with the relaxation time $\mathcal{T}$ having the constant of its frequency dependence $\mathcal{T}_{0\rm Pb} = 300{\rm MeV}^2\cdot$ s as explained in the text and in the Figures [51]; the quantities $k_{S,0}$, ν_0, Q_0, τ_0 and D_0 are calculated with $L = 0$.

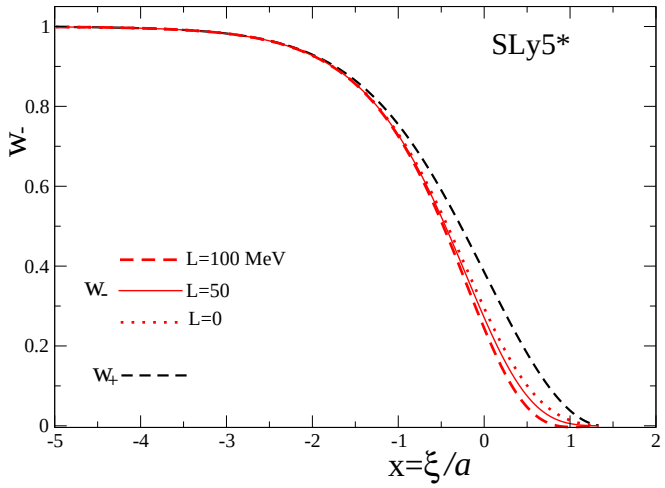

FIG. 1. (Color online) Isovector w_- (13) (with the relevant value of L Refs. [20, 41, 44]) and without ($L = 0$) derivative L constant, and isoscalar $w = w_+$ (see [7]) particle densities are shown vs $x = \xi/a$ for the Skyrme force SLy5* ($x \approx (r - R)/a$ for small nuclear deformations [31, 36, 43]).

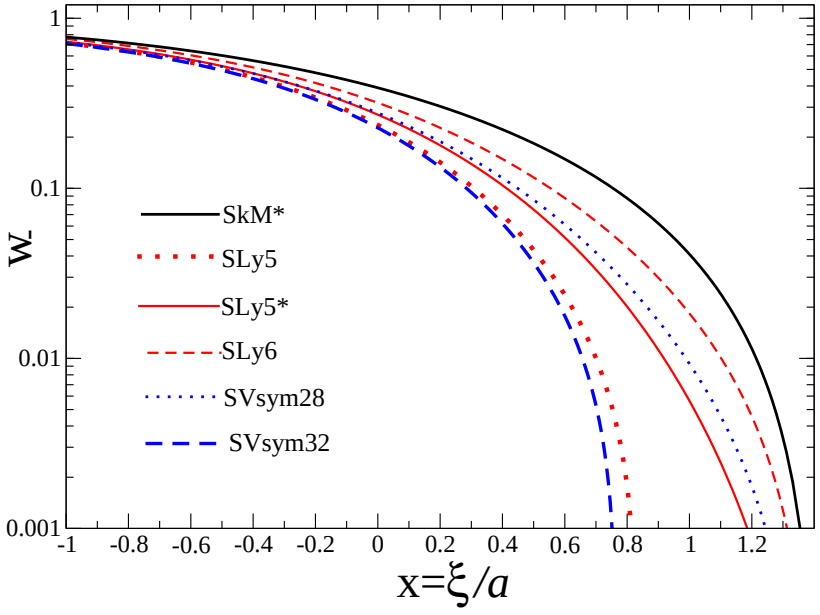

FIG. 2. (Color online) Isovector density $w_-(x)$ (13) (in the logarithmic scale) as function of x within the quadratic approximation to $e_+[\epsilon(w)]$ for several Skyrme forces [20, 37, 41, 43, 44].

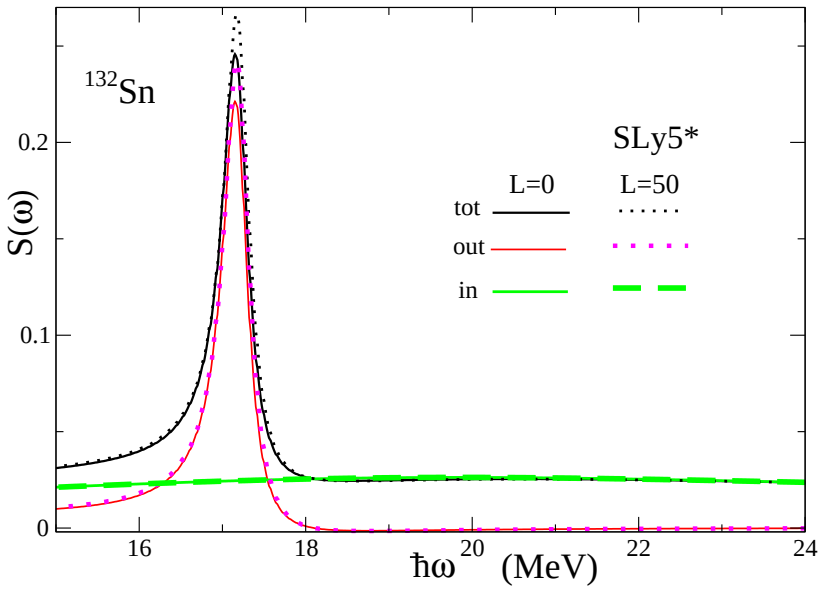

FIG. 3. (Color online) IVDR strength functions $S(\omega)$ vs the excitation energy $\hbar\omega$ are shown for vibrations of the nucleus ^{132}Sn for the Skyrme force SLy5* by dots and dashed lines at $L = 50$ MeV and solid lines for $L = 0$; red or magenta ("out-of-phase"), and green ("in-phase") curves show separately the main and satellite excitation modes, respectively (section 4 and 5); the collision relaxation time $\mathcal{T} = 4.3 \cdot 10^{-21}$ s in agreement with the IVGDR widths [51].

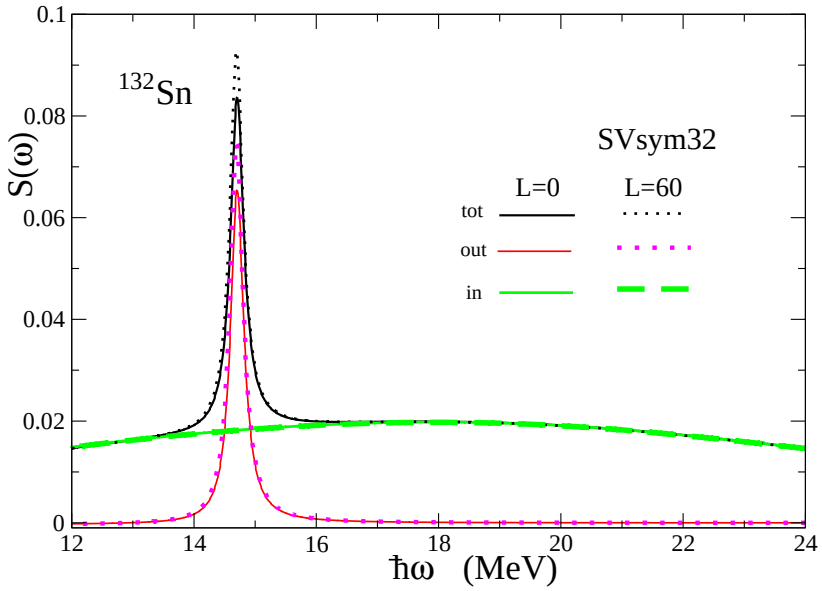

FIG. 4. (Color online) The same total and different modes (main and satellite) strengths as in Fig. 3 are shown for different $L = 0$ and 60 MeV for the Skyrme force SVsym32.

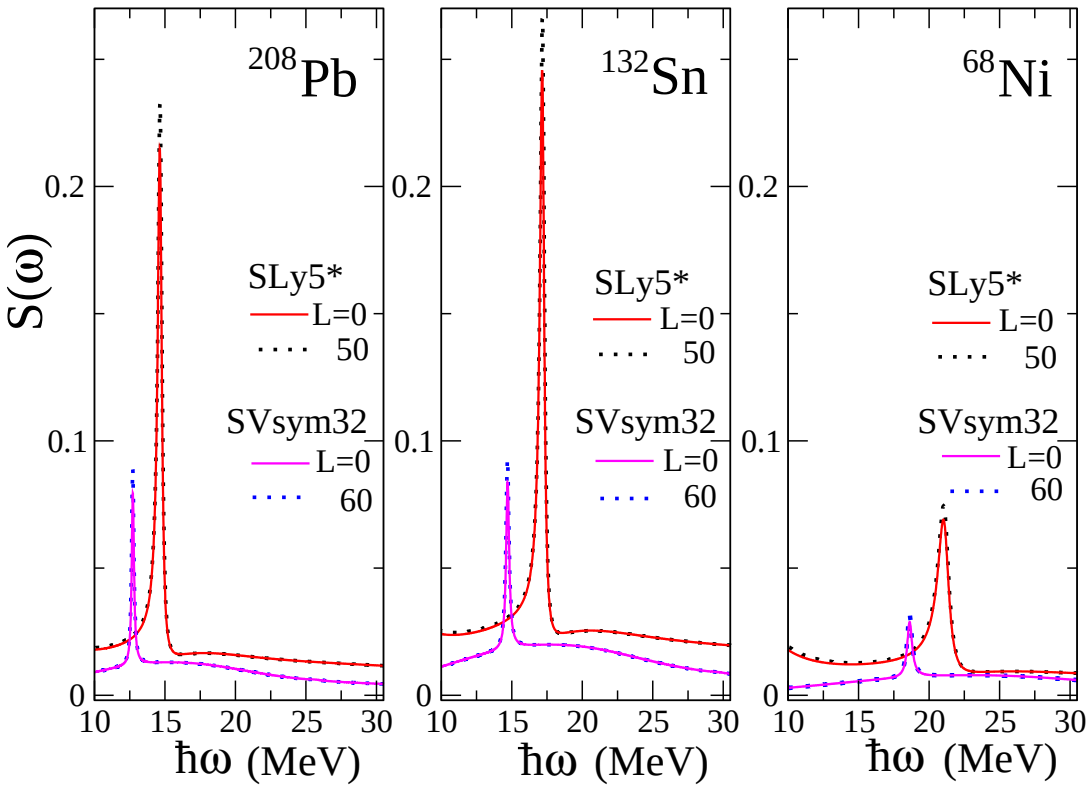

FIG. 5. (Color online) The total IVDR strength functions $S(\omega)$ vs the excitation energy $\hbar\omega$ (in MeV) for different double magic nuclei for SLy5* and SVsym32 forces; a slight dependence on the slope parameter L (in MeV) as compared to the $L = 0$ case at the main peaks is shown.

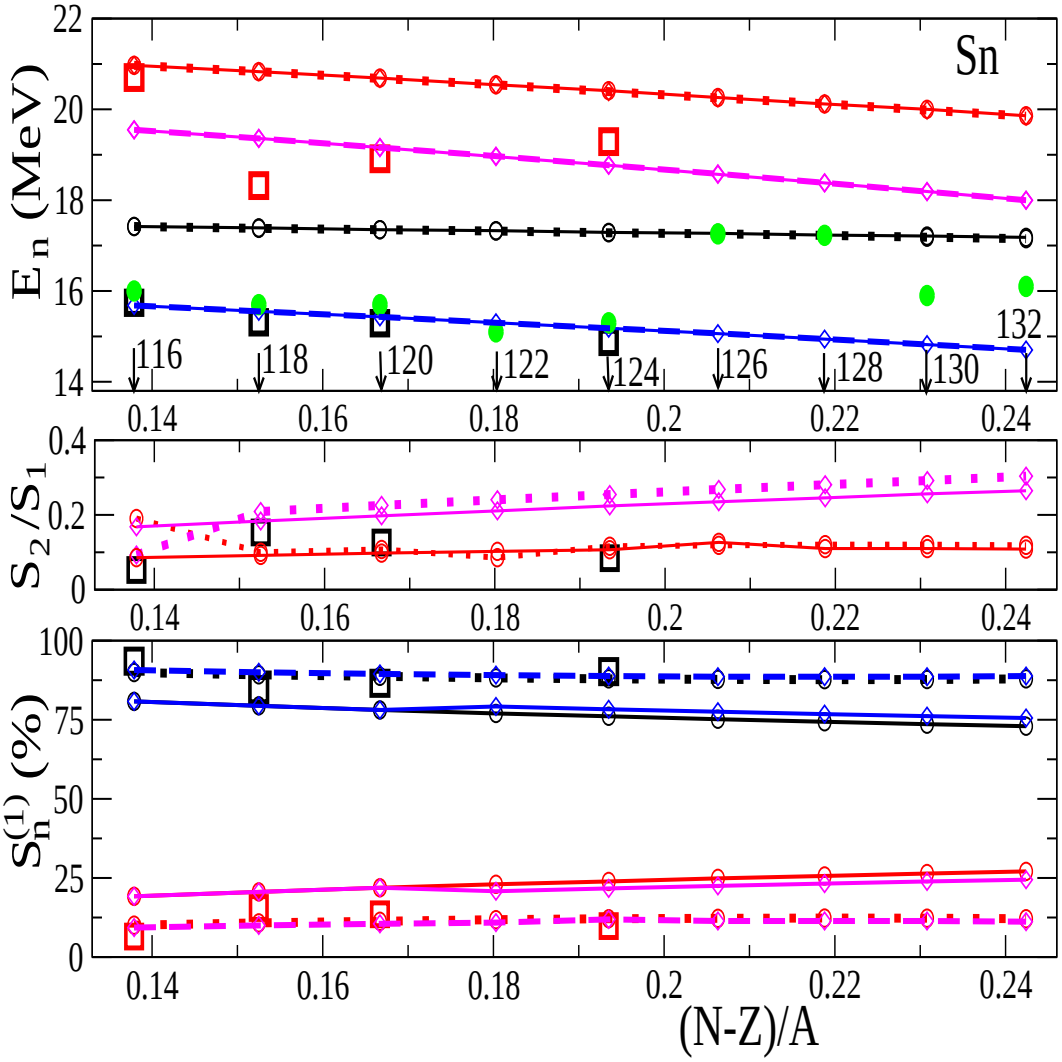

FIG. 6. (Color online) The IVDR splitting vs the asymmetry parameter $I = (N - Z)/A$. *Top:* the energies E_n of the main peak ($n = 1$) and satellite ($n = 2$); black ($n = 1$) and red ($n = 2$) open squares are obtained from the experimental data for the integral cross sections of Refs. [54–58] for several Sn isotopes, as explained in the text [30]; the solid and dotted black lines with opened circles are the main L=50 MeV and 0 peaks for SLy5* , respectively; the same red curves show the satellites; the solid and dashed blue lines with open diamonds denote the main L=60 MeV and 0 peaks for SVsym32* , respectively; the same margenta curves show the satellites; the green dots stands for the averaged (IVGDR) experimental data (three last from Adrich et al. [32]) and arrows show the particle number of the Sn isotopes. *Middle:* The ratio of the strengths at the satellite to those at the main peak, $S_n = S(\omega_n)$ (black solids and red dots for SLy5*; blue solids and margenta dashed curves for SVsym32); *Bottom:* The $S_n^{(1)}$ normalized to 100% as explained in the text with the same notations as in the top plot.

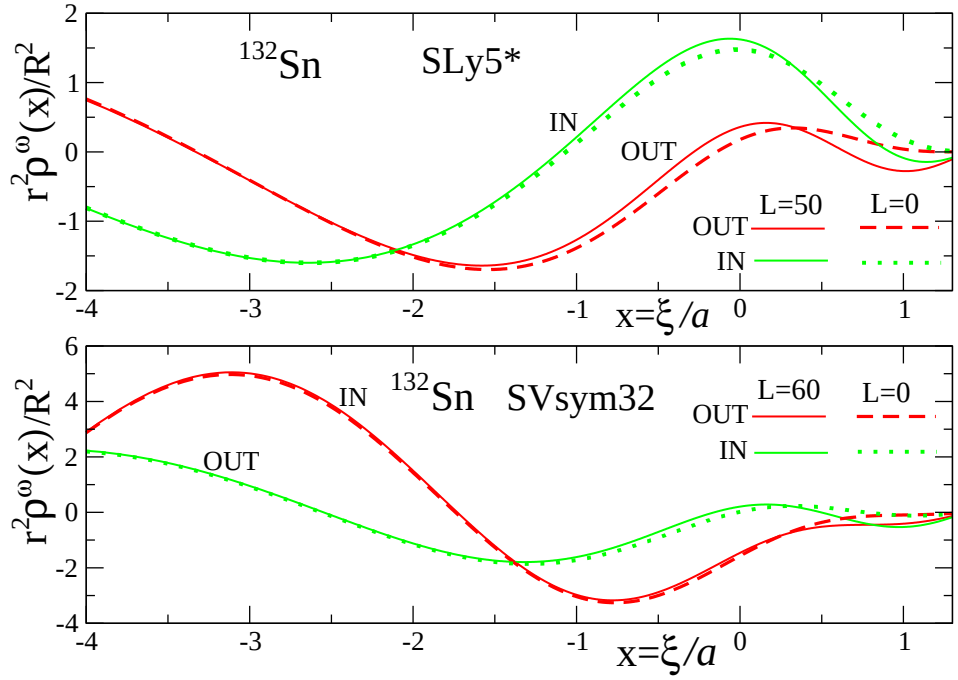

FIG. 7. (Color online) The IVDR main out-of-phase ($\delta\rho_-$, "out") and in-phase ($\delta\rho_+$,"in") transition densities $\rho^\omega_\pm(x)$ [Eq. (33)] multiplied by $(r/R)^2$, vs $x = \xi/a \approx (r-R)/a$ (spherical nuclei) for the satellite in ^{132}Sn with the Skyrme forces SLy5* [43] (upper panel) and SVsym32 [41] (lower panel); the two characteristic values $L = 0$ and $L = 50$ (or 60) MeV are shown; the relaxation time $\mathcal{T}$ is the same as in Fig. 3.

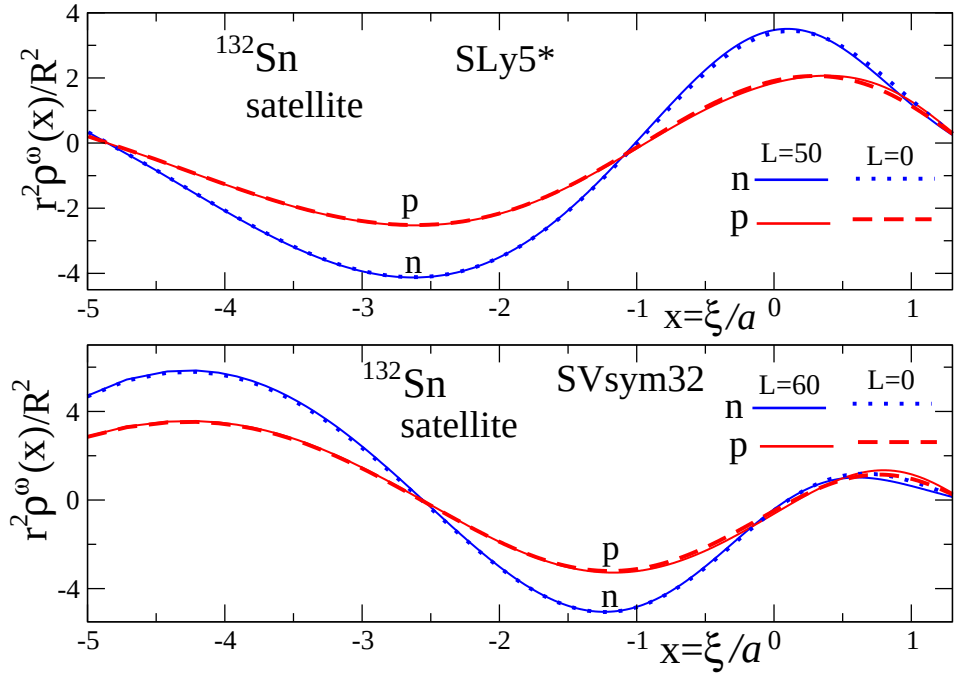

FIG. 8. (Color online) The same but for the IVDR neutron (n) and proton (p) transition densities $\rho^\omega(x)$ [Eq. (33)] multiplied by $(r/R)^2$, vs $x = \xi/a \approx (r-R)/a$ for the satellite at the energy E_2 in ^{132}Sn with the Skyrme forces SLy5* [43, 44] (upper panel) and SVsym32 [41] (lower panel); the two characteristic values $L = 0$ and $L = 50$ (or 60) MeV are shown too; the relaxation time $\mathcal{T}$ is the same as in Fig. 3.

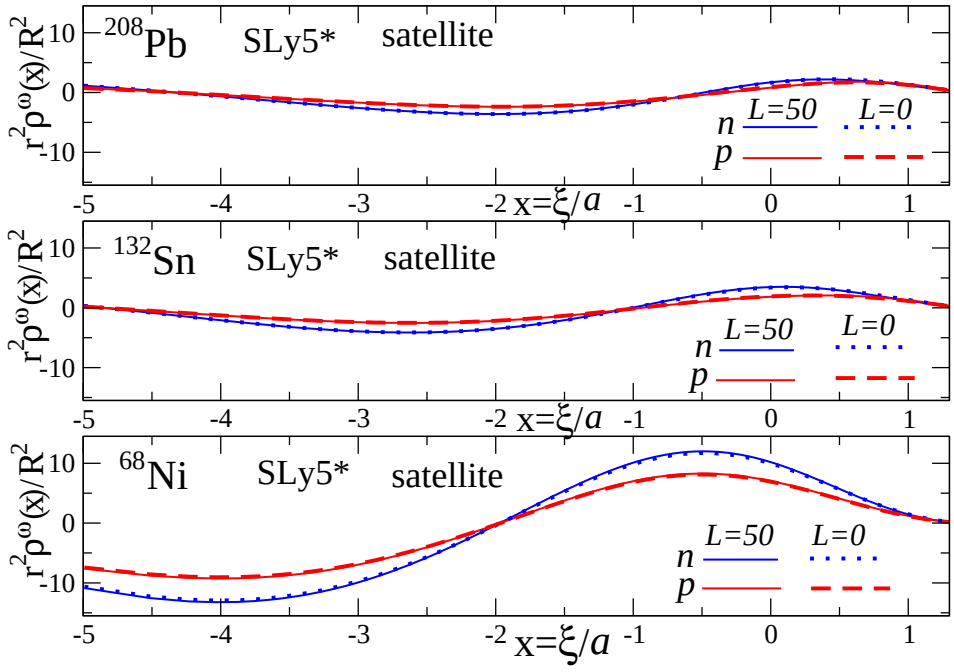

FIG. 9. (Color online) The IVDR n-p transition densities $\rho^{\omega}(x)$ multiplied by $(r/R)^2$ vs the dimensionless distance parameter $x = \xi/a \approx (r - R)/a$ for the same double magic nuclei slightly depending on the slope parameter L (in MeV) for a given example SLy5* of the Skyrme forces as compared to the $L = 0$ case near the ES edge as in Fig. 8.

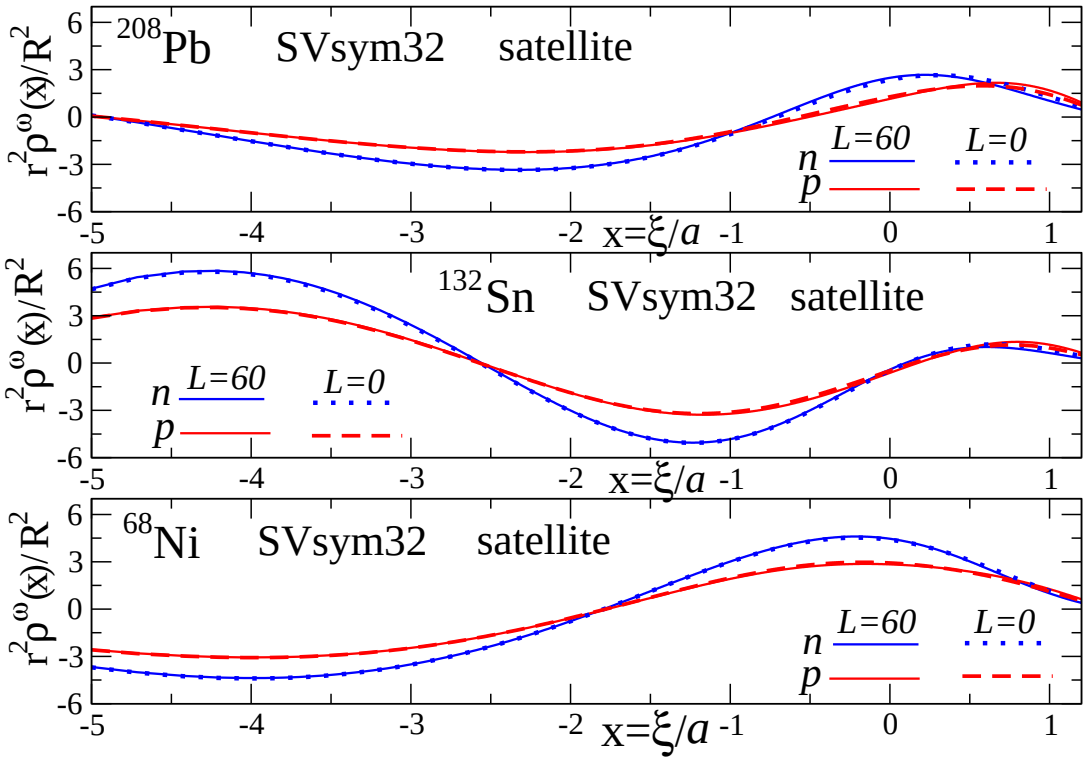

FIG. 10. (Color online) The same as in Fig. 9 but for the Skyrme force SVsym32.

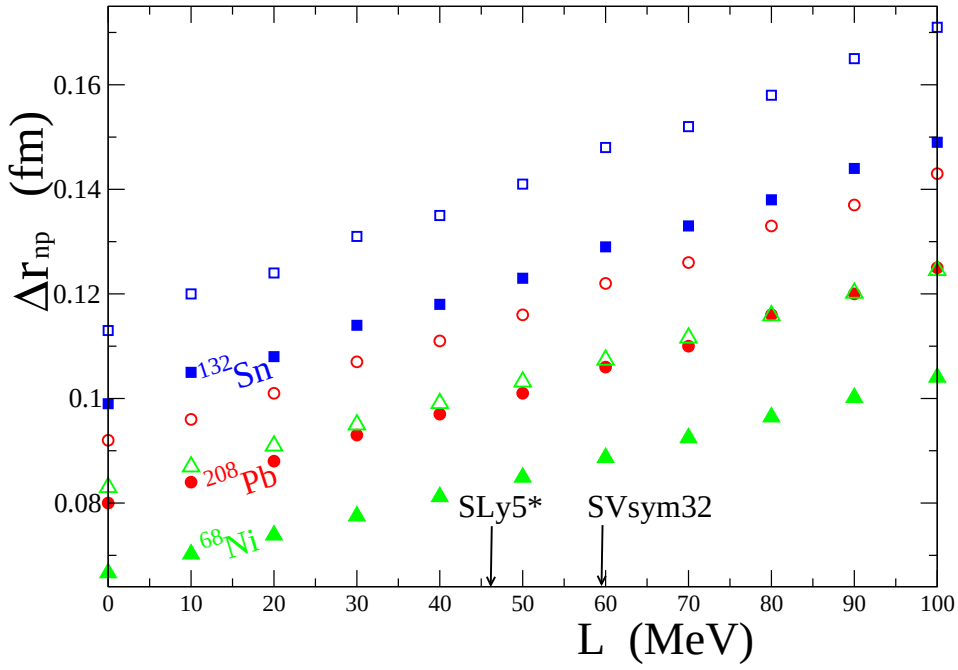

FIG. 11. (Color online) Neutron skin thickness $\Delta r_{np} = \sqrt{3/5}\ (R_n - R_p) = \sqrt{3/5}\ r_0\tau$ ($r_0 = 1.14$ fm) as a function of the derivative constant L for the same isotopes as in Table II and Figs. 5, 9 and 10 for the SLy5* and SVsym32 forces; full symbols show SLy5* and open ones correspond to SVsym32 calculations; arrows show approximately the values of L for different Skyrme forces taken from Refs. [41, 44].